The LS-TaSC™ Tool

Topology and Shape Computations

Example Problems

Version 4.2

Corporate Address
Livermore Software Technology, an Ansys Company
P. O. Box 712
Livermore, CA 94551-0712

Support Addresses
Livermore Software Technology, an Ansys Company
7374 Las Positas Road
Livermore, CA 94551-0712
T: 925 449 2500
F: 925 449 2507
E: sales@lstc.com
W: www.lstc.com

Livermore Software Technology, an Ansys Company
1740 West Big Beaver Road, Suite 100
Troy, MI 48084-3507
T: 248 649 4728
F: 248 649 6328

Contents

1. EXAMPLE PROBLEMS

The applications of the topology code is demonstrated with the help of a few test examples below. The examples are supplied together with the software executables (manual_examples.tar).

1.1. Fixed Beam with Central Load

This example demonstrates

1. how to define a problem,
2. how to add a load case,
3. how to define the design part,
4. how to run the problem, and
5. the analysis of the results.

The related files are available in MANUAL/Beam.

1.1.1. Problem Description

This example simulates a beam that is fixed on both ends. A pole with assigned initial velocity of 10m/s hits the beam in the center. The design part is meshed using 5mm^3 brick elements. The symmetry of the problem is used to design only half-section of the beam. The geometry and loading conditions of the beam are shown in Figure 1-1.

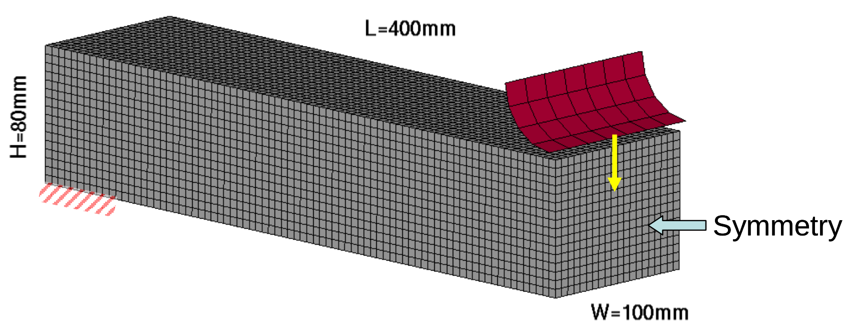

Figure 1-1: Geometry and loading condition.

1.1.2. Problem Setup

The project input data is saved to the file *beam.lstasc* as provided in the examples distribution. First, the *Case* icon from the main LS-TaSC GUI has to be selected, Figure 1-2. Specify the name of the load case, the LS-DYNA input file *Beam.dyn* and the LS-DYNA executable. The next step is to define the part to be optimized, Figure 1-3. Select the design part ID 101 and a desired mass fraction of 0.25. A maximum of 30 iterations are selected to find the optimal topology, Figure 1-4. Then run the optimization, Figure 1-5.

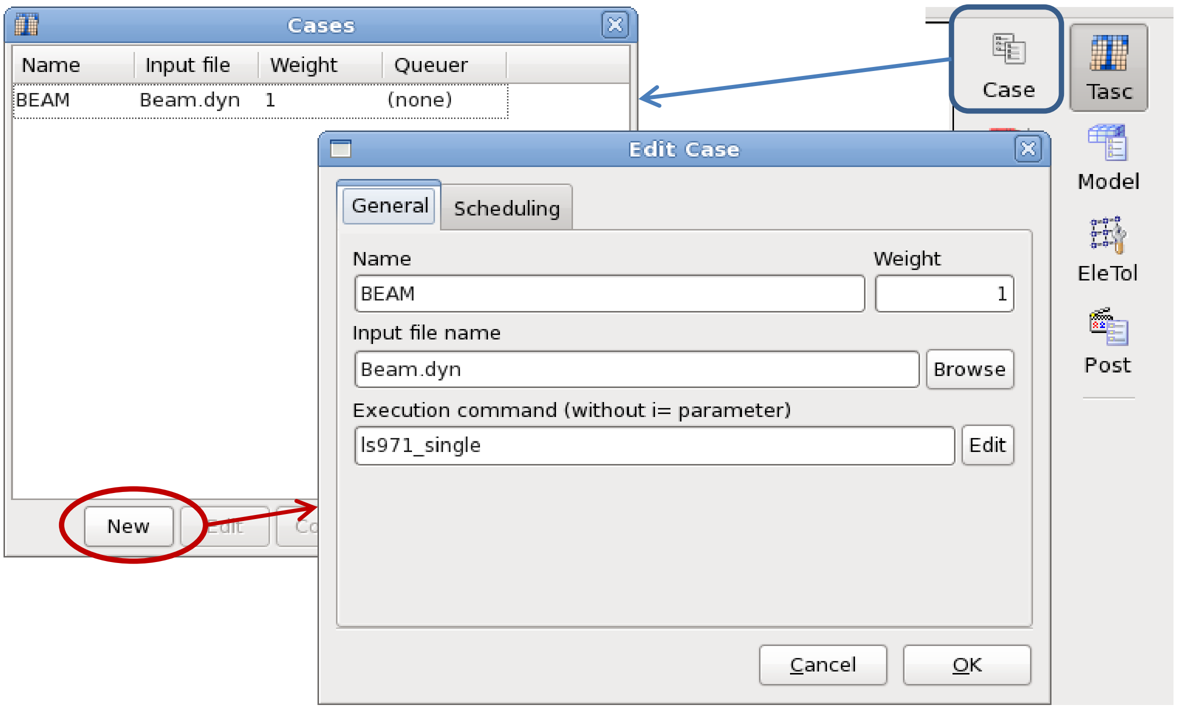

Figure 1-2: Definition of load case; specification of load case name, LS-DYNA input file and execution command.

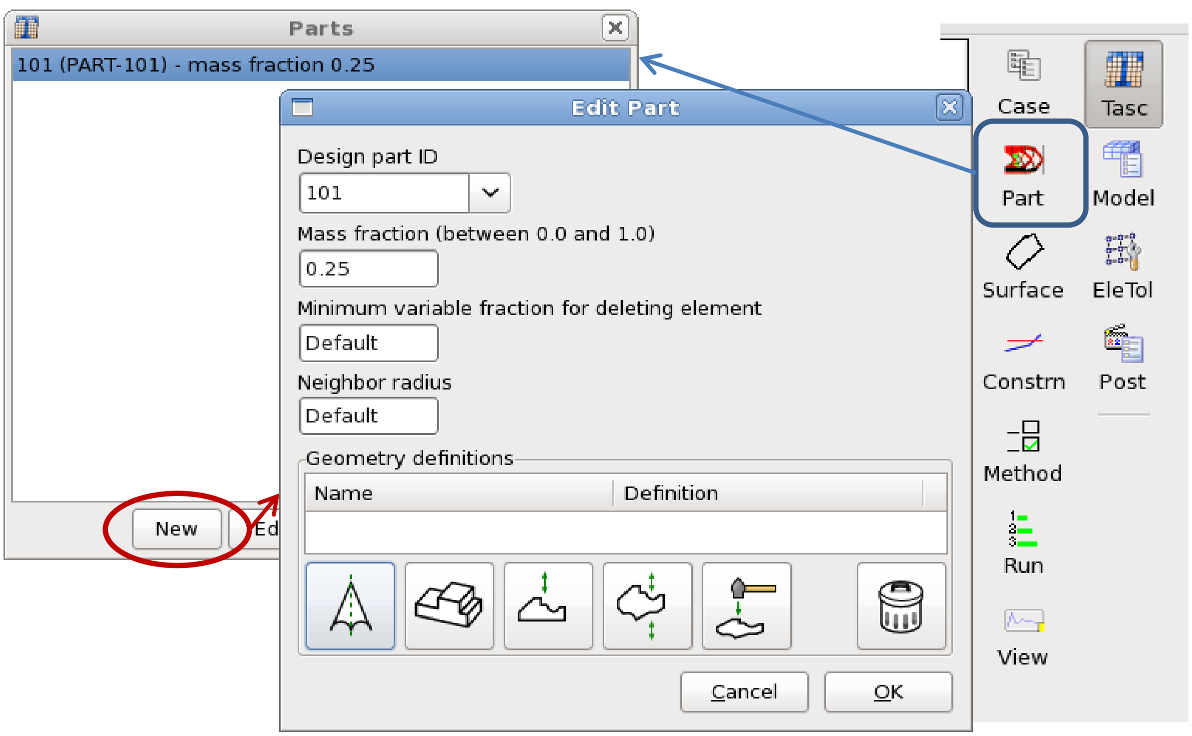

Figure 1-3: Definition of design part; specification of design part ID and desired mass fraction.

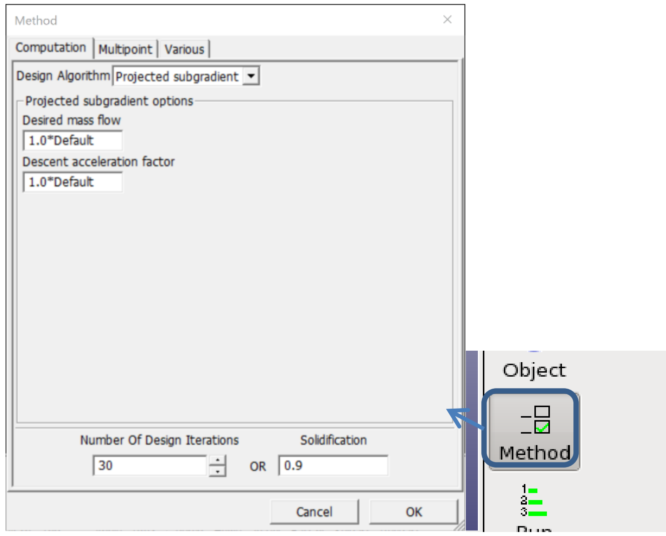

Figure 1-4: Definition of maximal number of iterations.

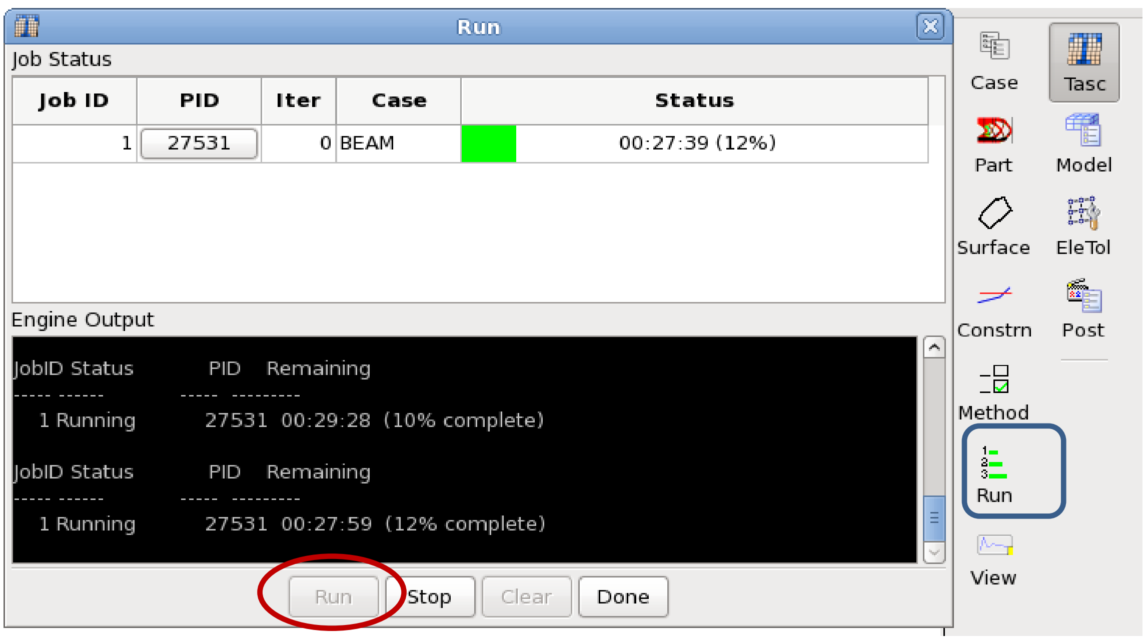

Figure 1-5: Run dialog

1.1.3. Results

The optimization converged after 22 iterations. The results can be visualized using the Topology history and Model plot options available in the *View* dialog, Figure 1-6.

The convergence is quantified using the fraction of the elements which is either fully used or deleted, characterized by the solidification as shown in Figure 1-7.

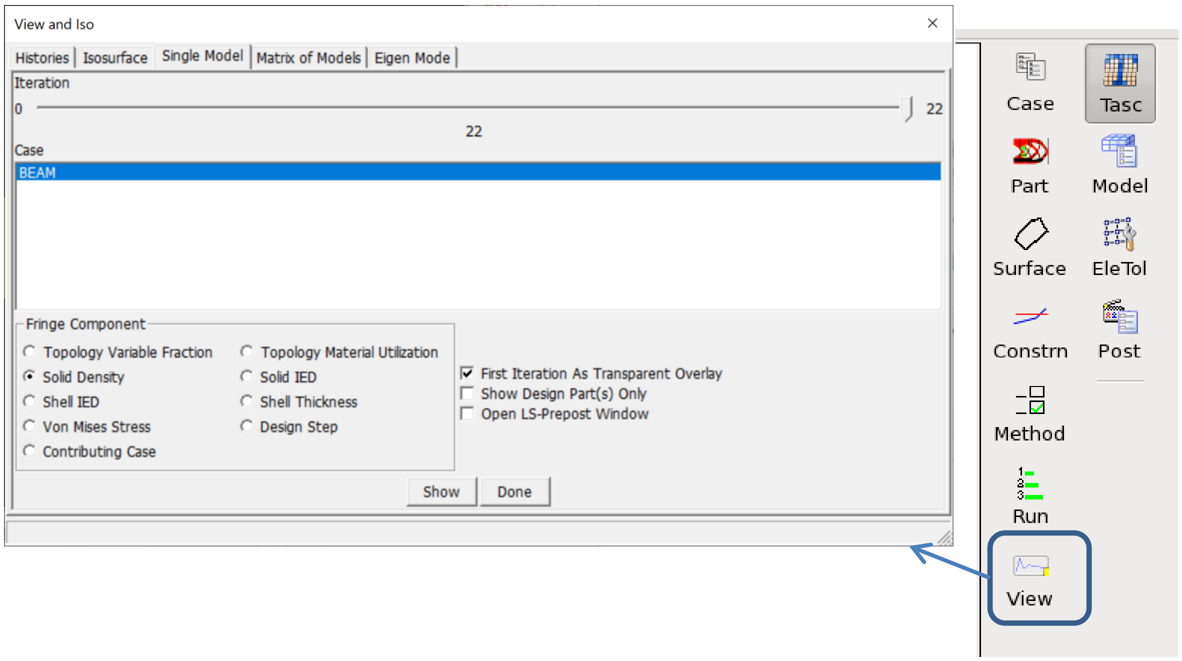

Figure 1-6: View dialog, visualization of optimization results

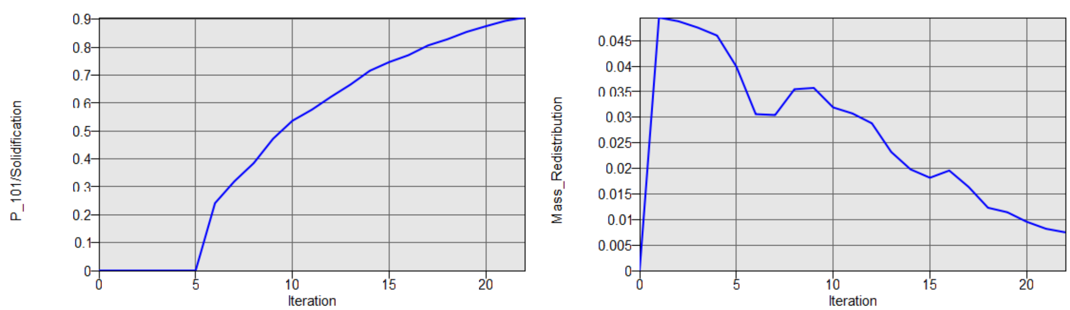

Figure 1-7: Topology history solidification and mass redistribution

The final topology is visualized in Figure 1-8. The topologies at different iterations during the evolution process are shown in Figure 1-9. The final topology evolved in a truss-like structure. Many holes were carved to satisfy the mass constraint while reducing the non-uniformity in the distribution of the internal energy density. The final structure was also found to have a reasonably homogenous distribution of the material as was desired. Topologies at different stages of the evolution process show that the main features of the structure were evolved by iteration 14. Further iterations were necessary to bolster the structure by removing the material from relatively non-contributing zones and redistributing it to the desirable sections such as a 0-1 type topology was evolved.

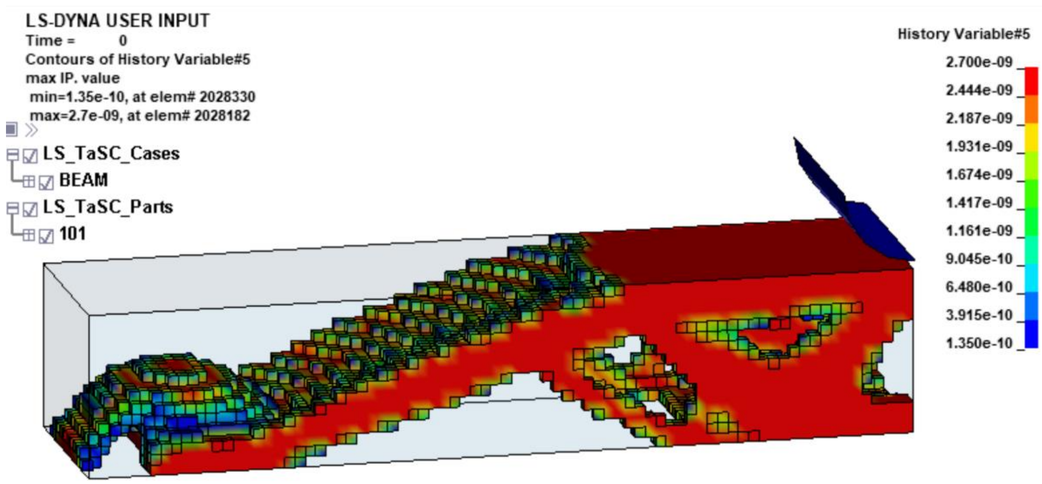

Figure 1-8: Initial and final design, fringe component solid density.

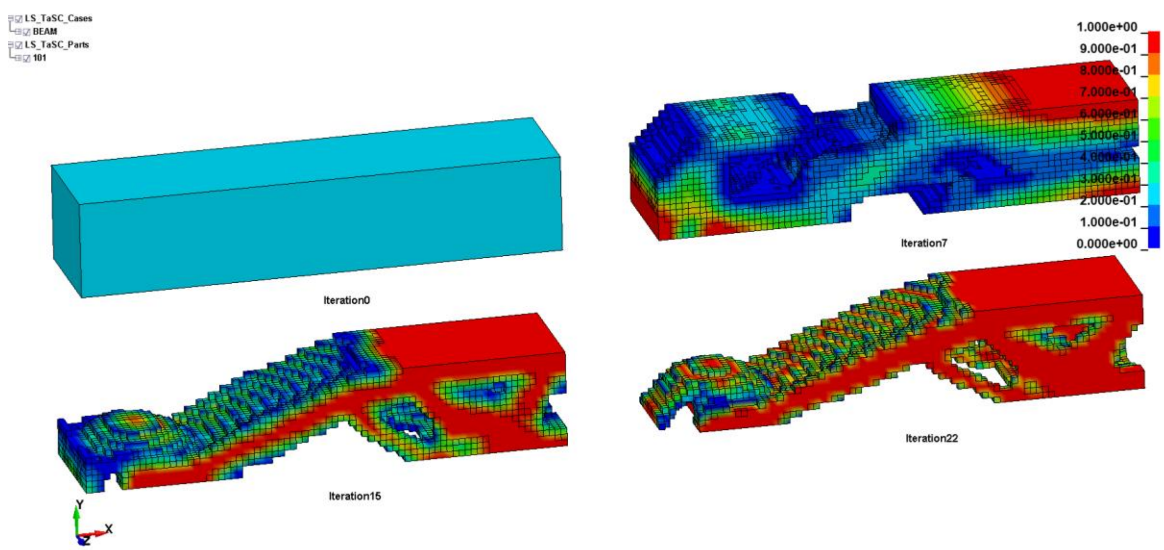

Figure 1-9: Evolution of the geometry shown using density contours.

1.2. Beam using geometry definitions

This example demonstrates

- how to set up a problem with extrusion definitions, and
- how to set up a problem with casting definitions.

The related files are available in MANUAL/Beam_extr_cast.

1.2.1. Problem Description

The same fixed-beam as described in section 1.1.1 is analyzed with extrusion and casting definitions. The symmetry face is also defined as the extruded face. In the input deck file, the

elements on the extrusion face were grouped in a solid set (*SET_SOLID). Two different casting conditions were applied in two separate design runs:
(i) in the first run casting definition was applied in the Z direction, and
(ii) in the second run a two-sided casting definition was applied in the Z direction.
All other parameters were kept the same.

1.2.2. Problem Setup

The project input data is saved to the file *Extr_Cast.lstasc* and *Extr_Cast2.lstasc* as provided in the examples distribution in the directory *Beam_extr_cast*. Additionally to the setup explained in section 1.1.2, the extrusion and casting definition has to be specified, Figure 1-10.

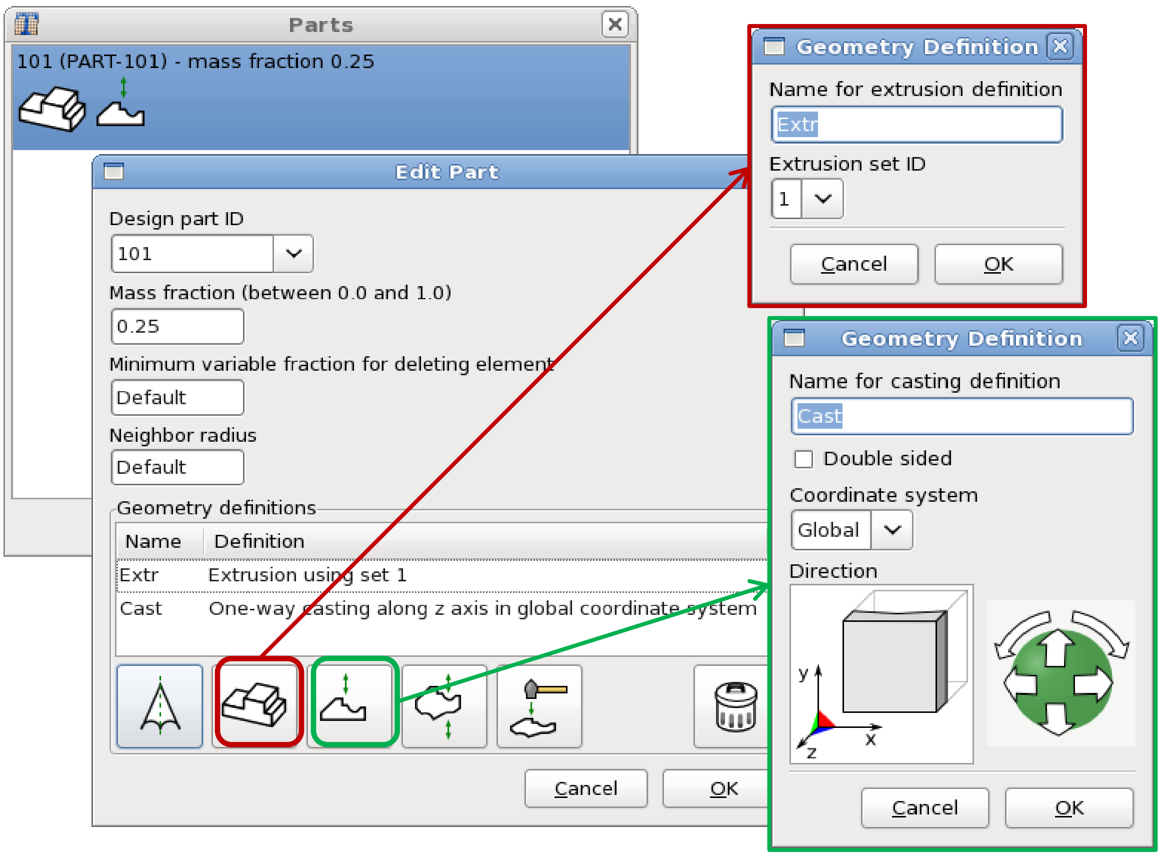

Figure 1-10: Definition of design part with extrusion and casting constraint.

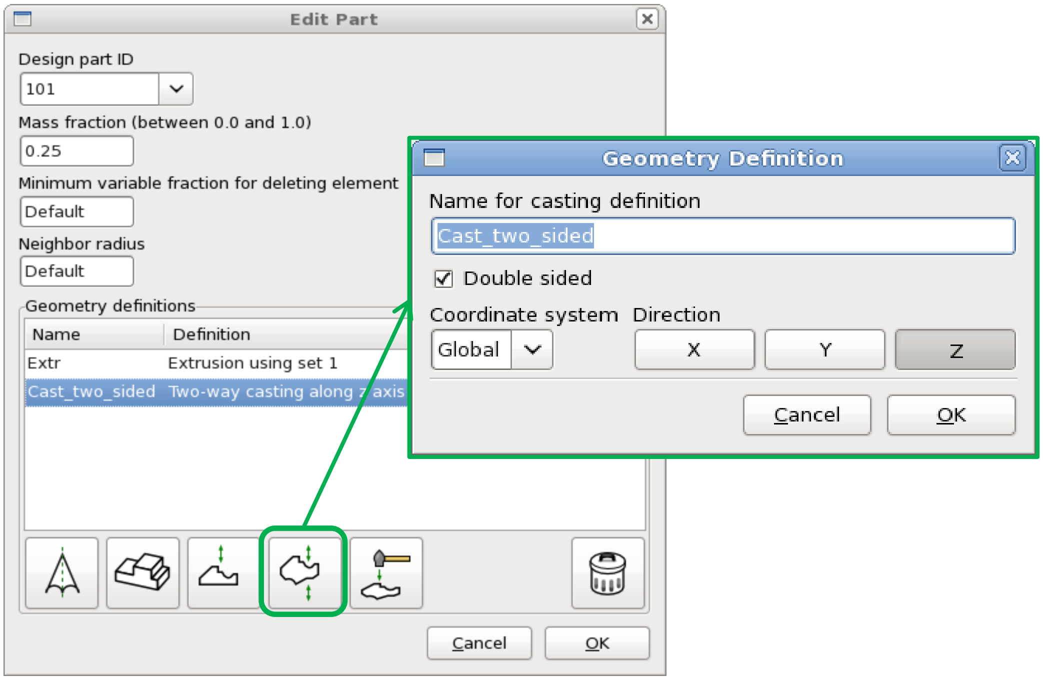

Figure 1-11: Definition of design part with extrusion and 2-sided casting constraint

1.2.3. Results with extrusion and casting

The optimization converged after 25 iterations. Different phases in the evolution are depicted in Figure 1-12. One can see that a lot of material was removed early. The final geometry evolved by considering the geometry definitions was significantly different than the case when no manufacturing constraints were considered. The C-section evolved makes intuitively sense.

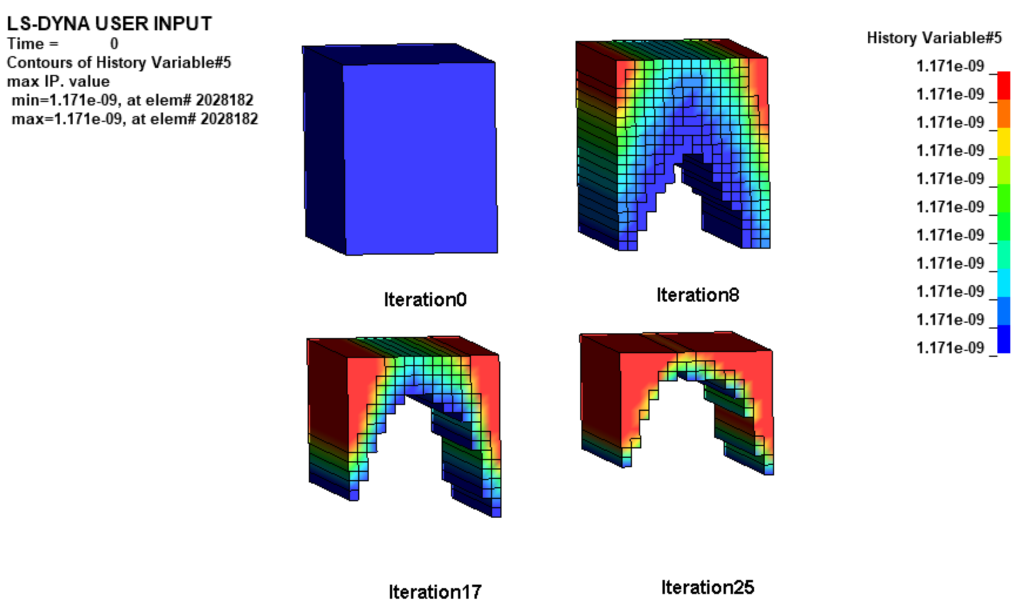

Figure 1-12: Evolution of the beam using extrusion and single-sided casting constraints

1.2.4. Results with extrusion and two-sided casting

Different phases in the evolution are depicted in Figure 1-13. One can see that a lot of material was removed early. The final geometry evolved by considering the geometry definitions was significantly different than the case when no manufacturing constraints were considered. The I-section evolved makes intuitively sense.

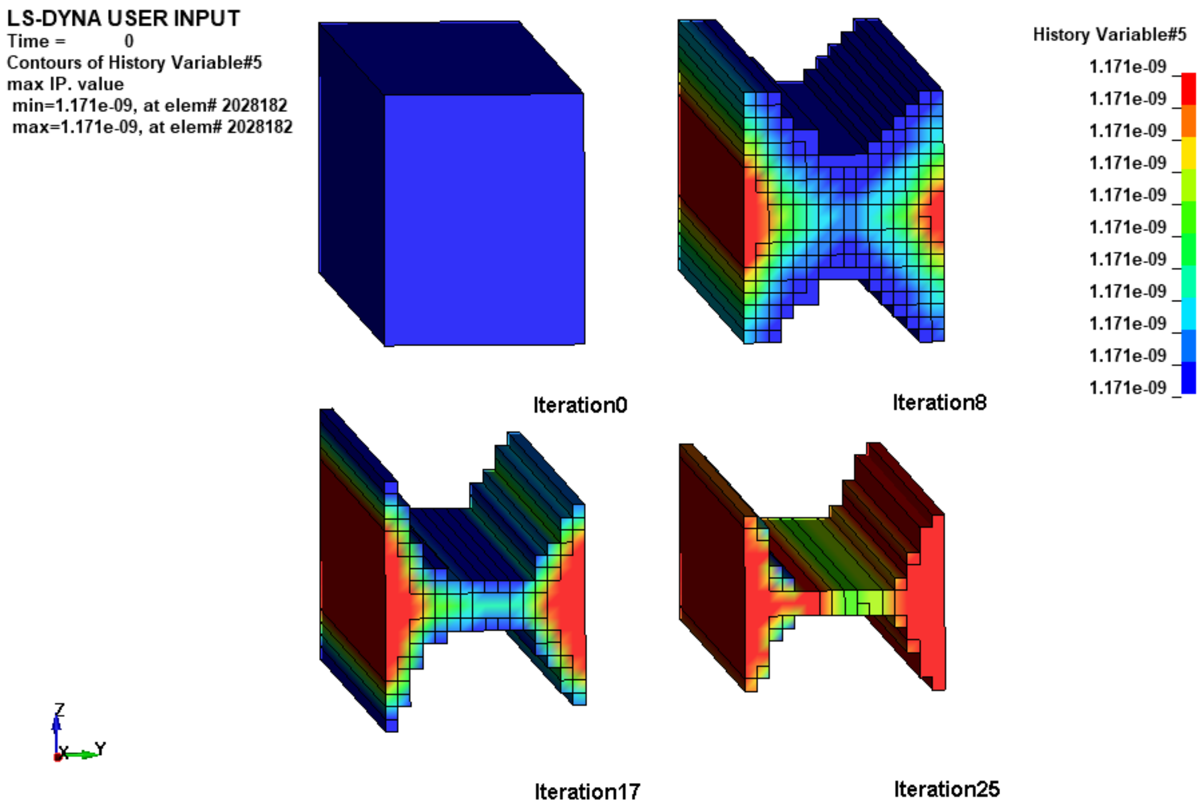

Figure 1-13: Evolution of the beam using extrusion and two-sided casting constraints.

1.3. Shell Example

This example demonstrates

- the optimization of a shell structure.

The related files are available in MANUAL/Shell.

1.3.1. Problem Description

The geometry and loading conditions for the example are shown in Figure 1-14.

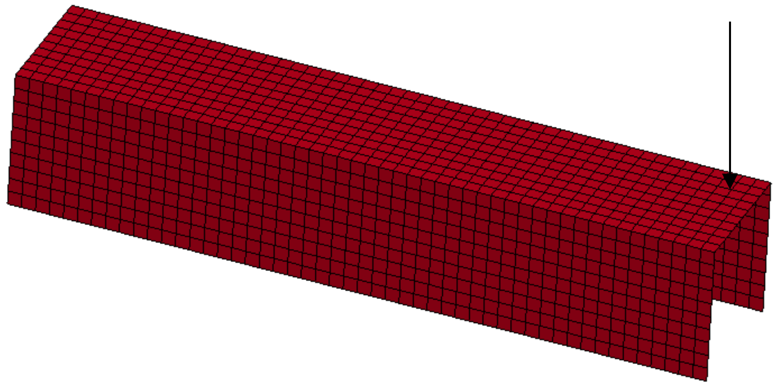

Figure 1-14: The geometry and loading conditions of the shell example. The left side is built-in, while a downward load is applied to the right, back corner.

1.3.2. Problem Setup

The project input data is saved to the file *Shell.lstasc* as provided in the examples distribution. The definition of the load case is displayed in Figure 1-14. The input file name and the LS-DYNA execution command has to be specified. Figure 1-16 shows the definition of the design part. The design part ID is 1 with a desired mass fraction of 0.3. The design algorithm Optimality criteria was used, since shell elements are optimized. The variable fraction for deleting elements was increased to 0.05. The convergence tolerance was set to 0.01, Figure 1-17.

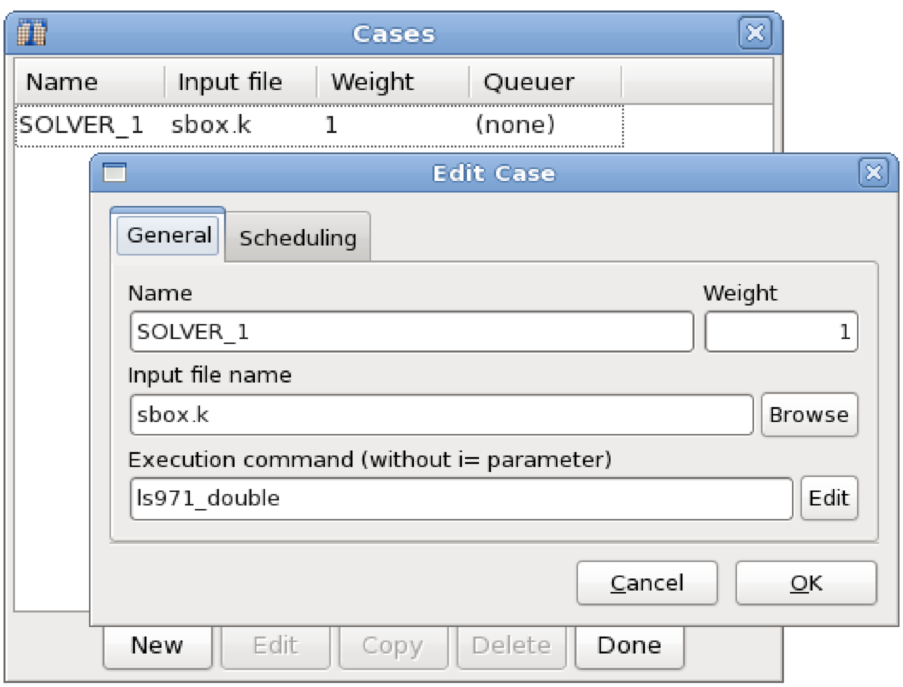

Figure 1-15: Definition of load case

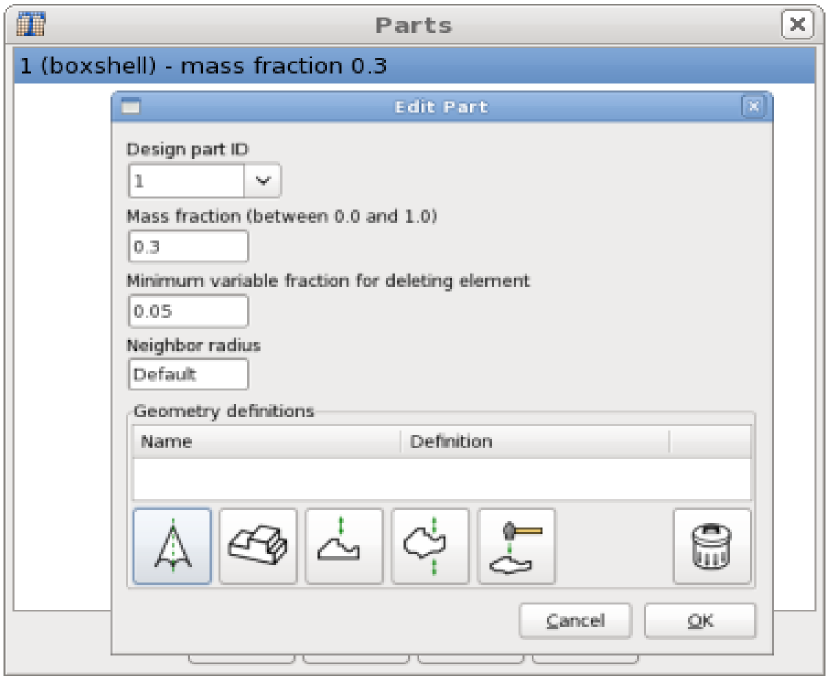

Figure 1-16: Definition of design part and mass fraction

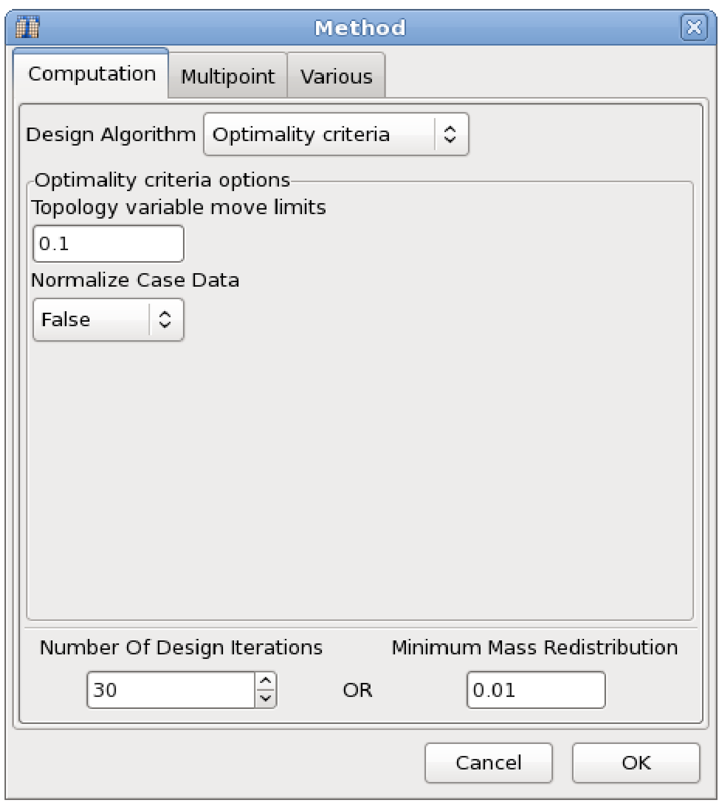

Figure 1-17: Method dialog; the Design Algorithm was set to Optimality criteria and the convergence tolerance was increased to 0.01

1.3.3. Results

The simulation converged after 12 iterations. The convergence history for the shell example is shown in Figure 1-18. There was largely monotonic reduction in the mass redistribution.

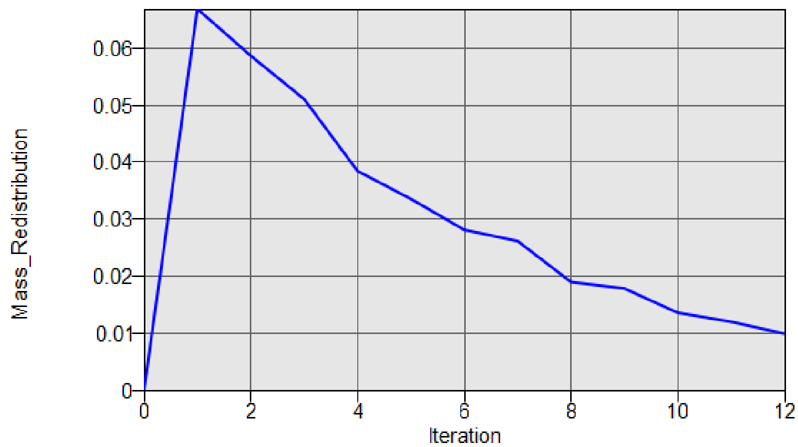

Figure 1-18: Mass Redistribution - Convergence history for the shell example.

The final design is shown in Figure 1-19. The final structure had many cutouts and resembled an optimized truss-like structure.

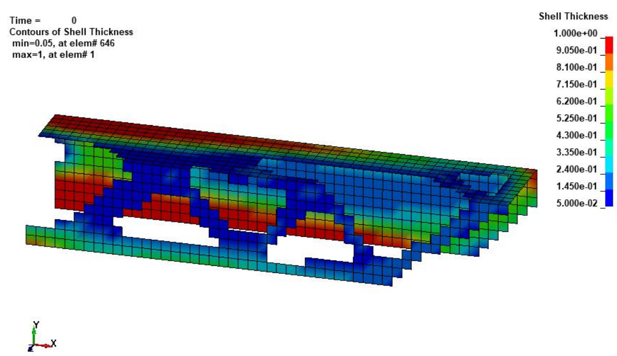

Figure 1-19: Shell thickness fringed on final geometry for the shell problem.

1.4. Simplified Side Impact

This example demonstrates

- the use of the multipoint scheme to solve constrained problems, and
- solving for multiple constraints by subdividing parts to create a stiffness gradient.

The related files are available in MANUAL/SideImpact.

1.4.1. Problem Description

The design problem here is that the intrusion constraints require that the B-pillar have a stiffness gradient. The geometry and loading conditions for the example are shown in Figure 1-20. One loadcases with two displacement constraints is considered. The part was subdivided into four parts thereby allowing us to specify a stiffness gradient from the top to the bottom using the four part mass fractions. The model has 60 000 elements.

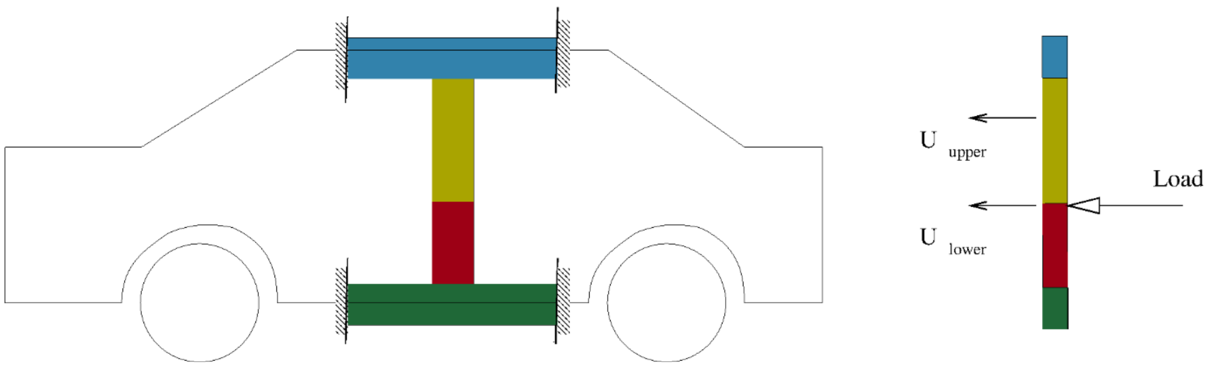

Figure 1-20: The geometry of the simplified side impact example showing all four design parts

The displacements are monitored at an upper and lower location. Two constraints are defined:

$$-10\, u_{lower} < 1$$
$$2u_{upper}/u_{lower} < 1$$

Because of element deletion, some intermediate responses are defined to ensure that a node with the desired displacement is found.

1.4.2. Problem Setup

The project input data is saved to the file *4mf.lstasc* as provided in the examples distribution. The definition of the design parts with mass fraction 0.3 is displayed in Figure 1-21. The definition of the constraints and the selection of the multipoint method is displayed in Figure 1-22.

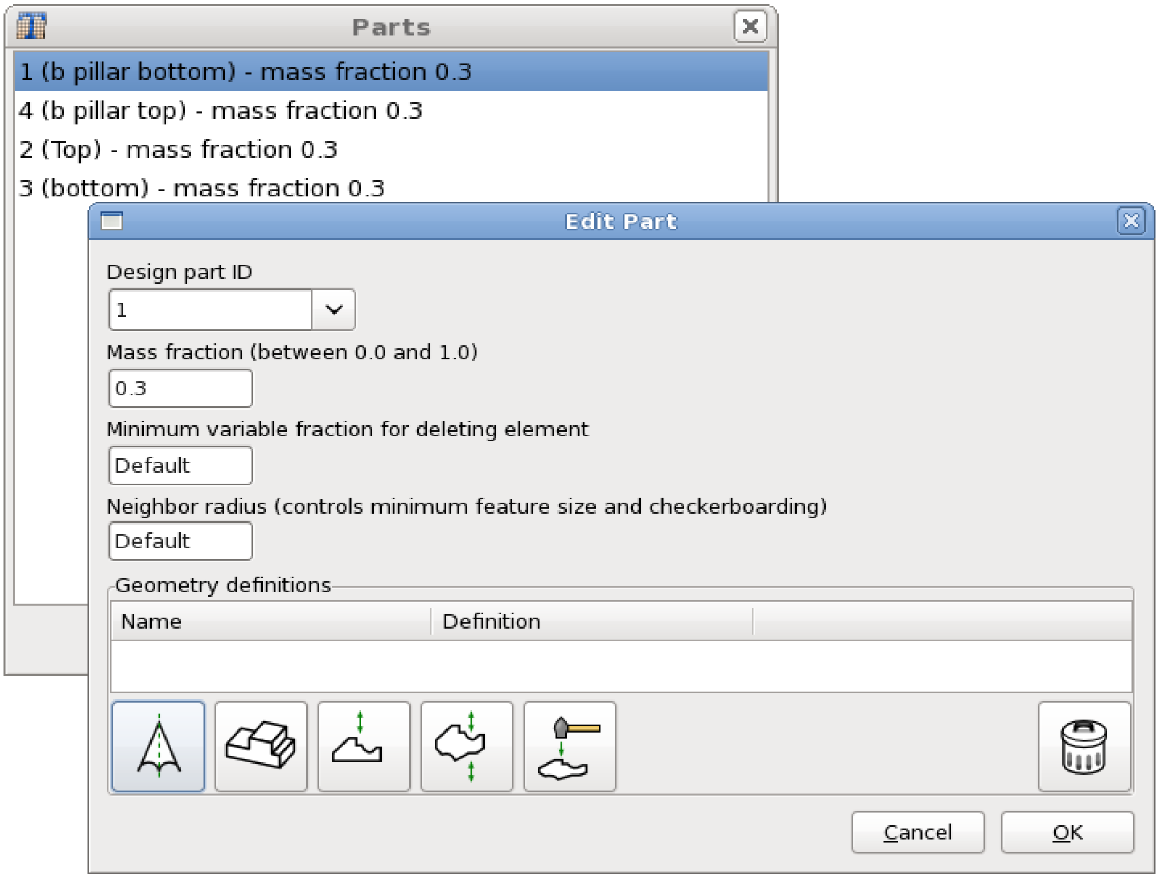

Figure 1-21: Definition of the four design parts

Figure 1-22: Definition of multipoint method and constraints.

1.4.3. Results

The optimization converges after 24 iterations. The histories for the mass fractions are shown in Figure 1-23, while Figure 1-24 shows the convergence of the constraint values. The iso-surface with iso-level 0.5 of the final design is shown in Figure 1-25.

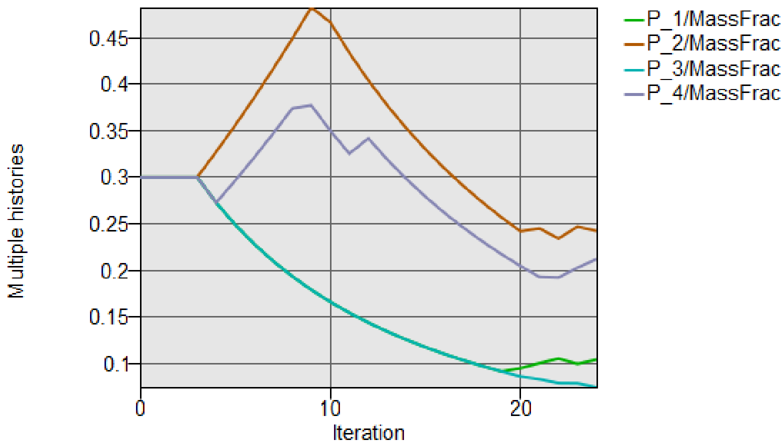

Figure 1-23: Convergence history – Mass Fractions

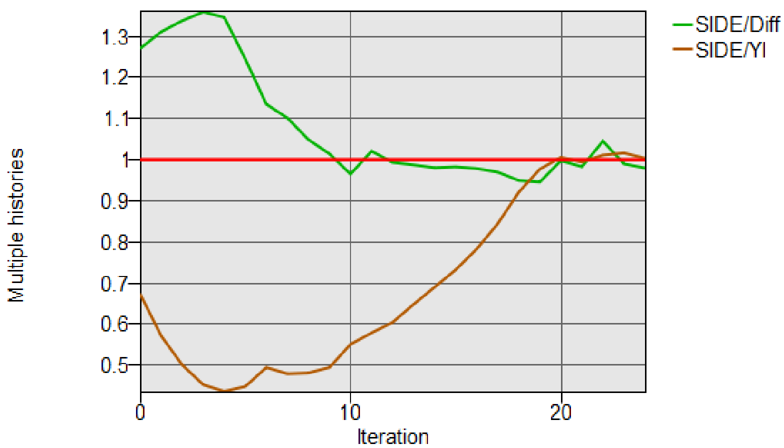

Figure 1-24: Convergence history – Constraint values

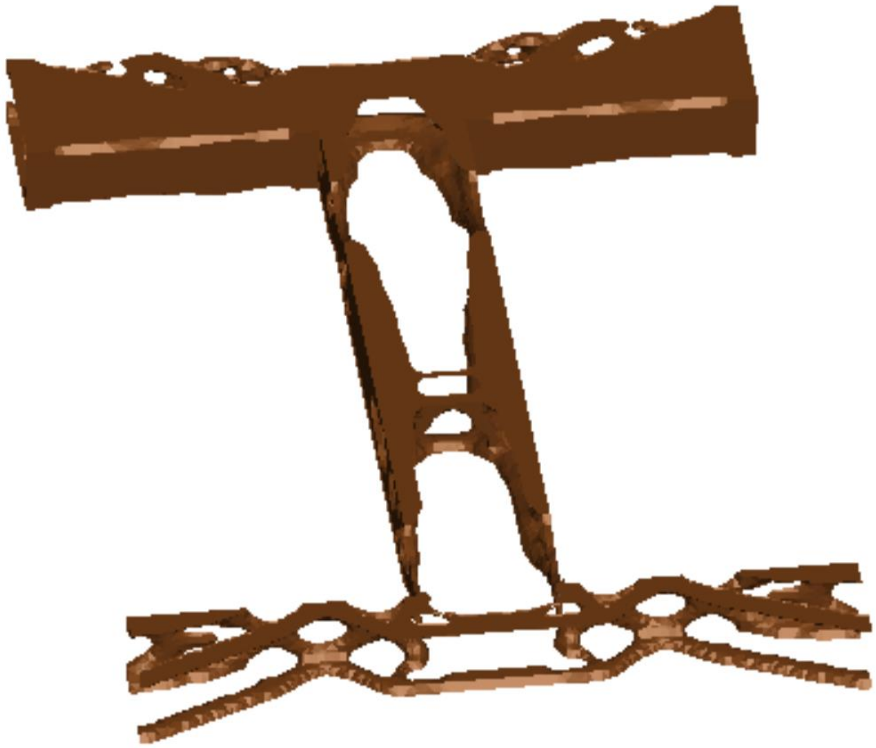

Figure 1-25: Final design for the simplified side impact problem: iso-surface with iso-level 0.5

1.5. Optimization of Multiple Load Cases

This example demonstrates

- optimization of multiple load cases,
- a symmetry geometry definition,
- constraints,
- dynamic weighting of load cases,
- constrained optimization using multi-point method and
- the projected subgradient algorithm.

The related files are available in MANUAL/MLC.

1.5.1. Problem Description

The geometry and loading conditions for the example are shown in Figure 1-26. This is a fixed-fixed beam with three loads. The three load cases were identified according to the location of the pole hitting the beam. The design part was meshed with $(10mm)^3$ elements.

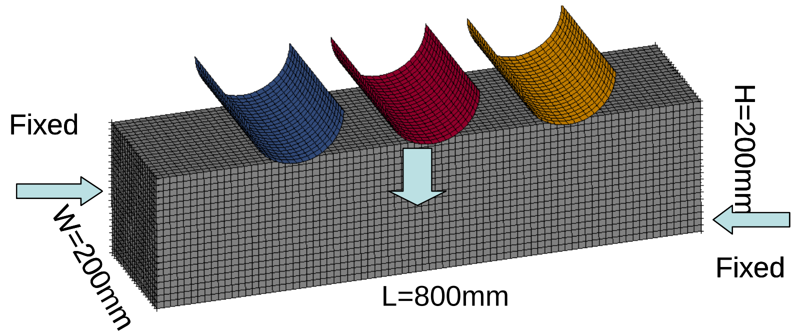

Figure 1-26: The geometry and loading conditions of the multiple load case example.

1.5.2. Problem Setup

Figure 1-26 displays the design part definition. The problem is symmetric, so only two load cases are therefore used and symmetry is defined, (Figure 1-27). The desired mass fraction for this example is 0.3. The maximal displacements at the centers of impact for both load cases are constrained to be less than 110, see Figure 1-28. A maximum of 50 iterations are allowed. All simulations of both load cases of an iteration are run simultaneously.

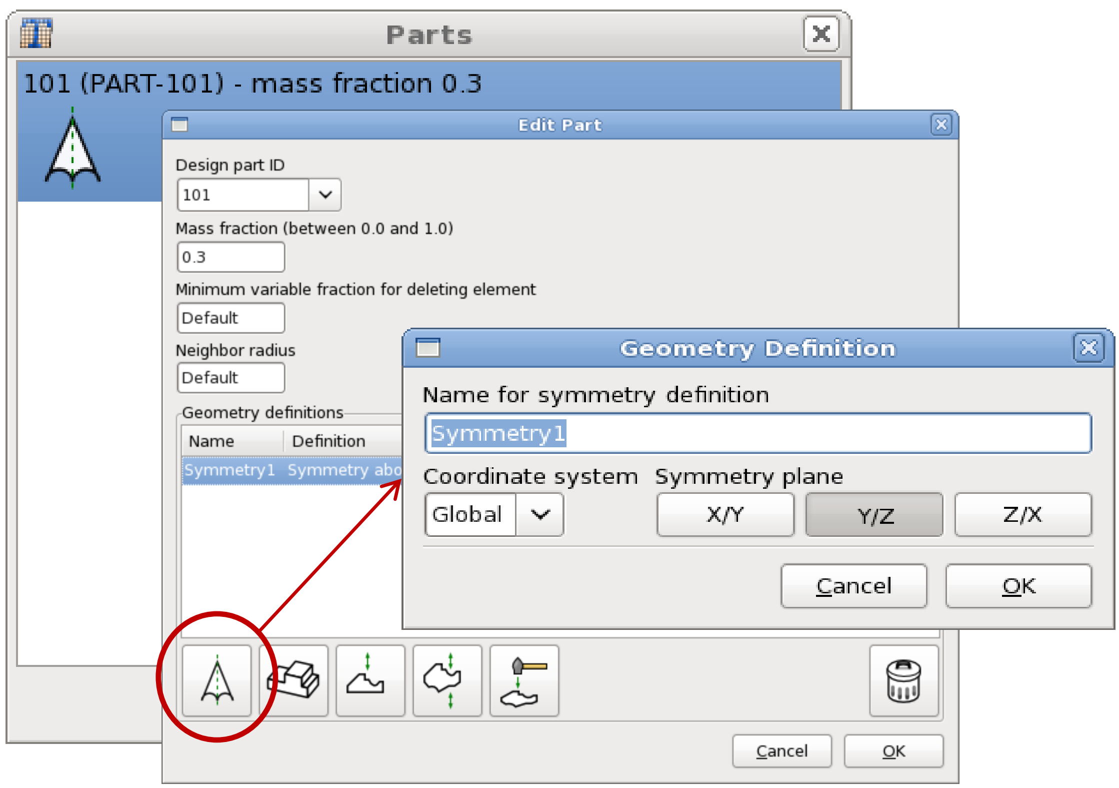

Figure 1-27: Definition of design part with symmetry condition and mass fraction 0.3.

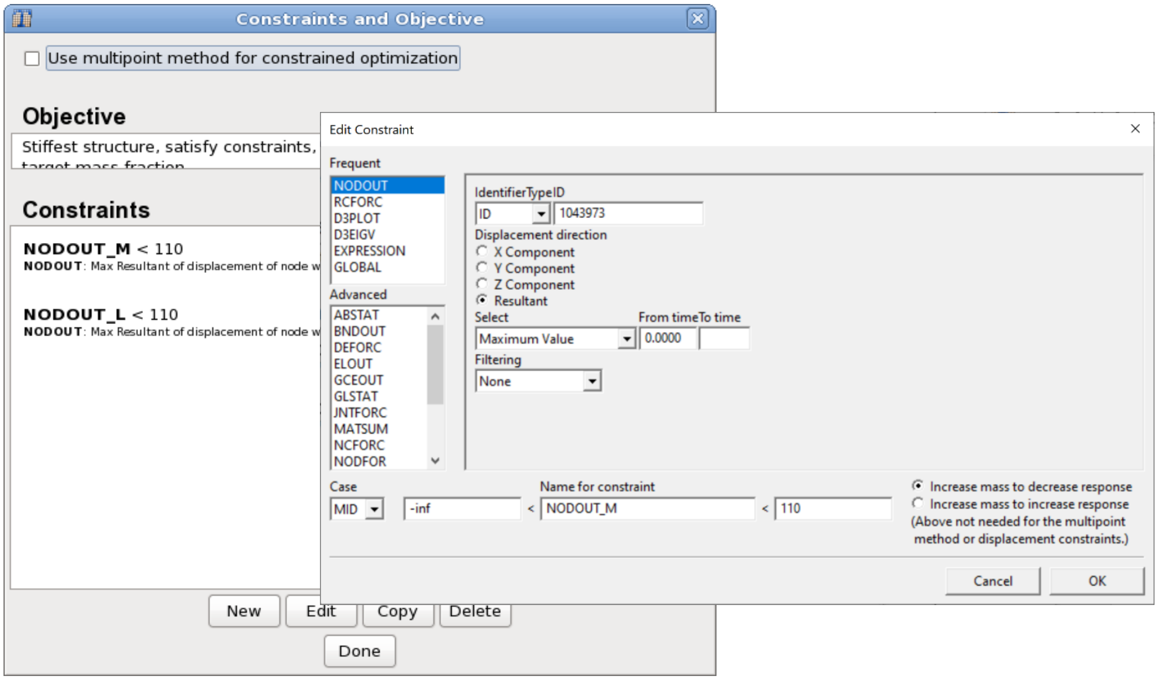

Figure 1-28: Definition of constraints – displacement of centers of impact < 110.

Two approaches to solve this optimization problem are executed. The problem is analyzed using dynamic weighting (*mlc_dynweight.lstasc*) of the load cases as well as the multi-point method (*mlc_multipoint.lstasc*).

Dynamic weighting can be activated in the *Weight* dialog accessible from the *Cases* dialog *Dynamic Weights* button, Figure 1-29. The multi-point method can be switched on in the *Constraints* dialog or *Method* dialog *Multipoint* tab, Figure 1-30. Forward differences are used to optimize the global variables, the mass fraction and the load case weights.

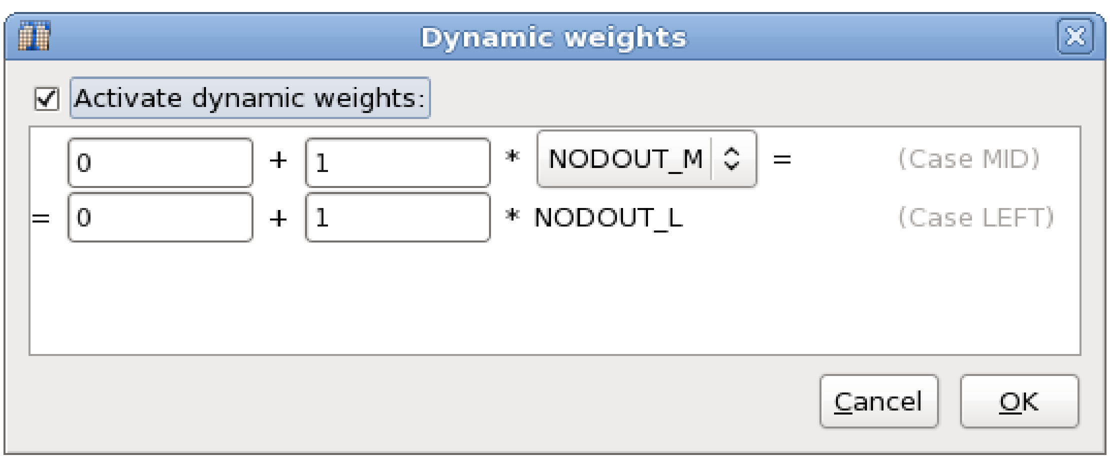

Figure 1-29: Definition of dynamic weights

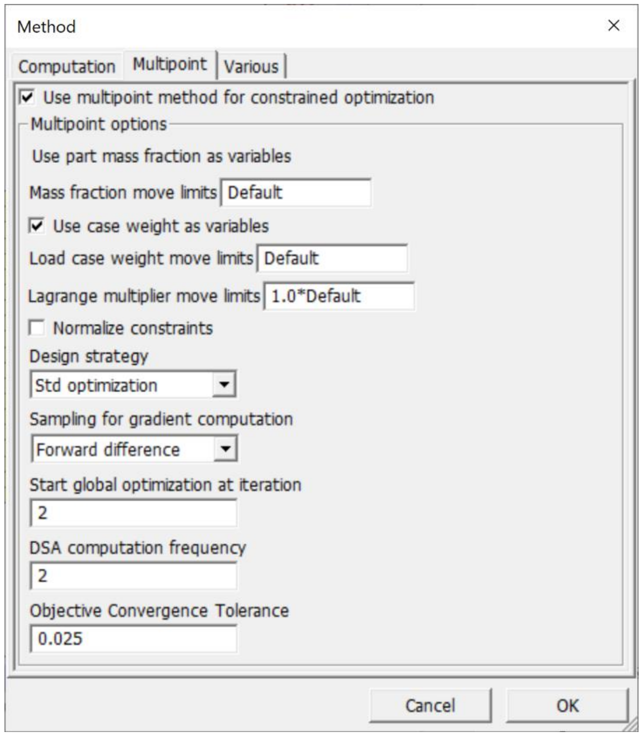

Figure 1-30: Settings for multipoint method

1.5.3. Results with dynamic weighing

The optimization converged after 49 iterations. The convergence history for the multiple-load example solved with dynamic weights is shown in Figure 1-31. Results are much improved by the dynamic weighting. The constraints are reasonably close to the bound as shown in Figure 1-31 due to the load case weighting computed also shown.

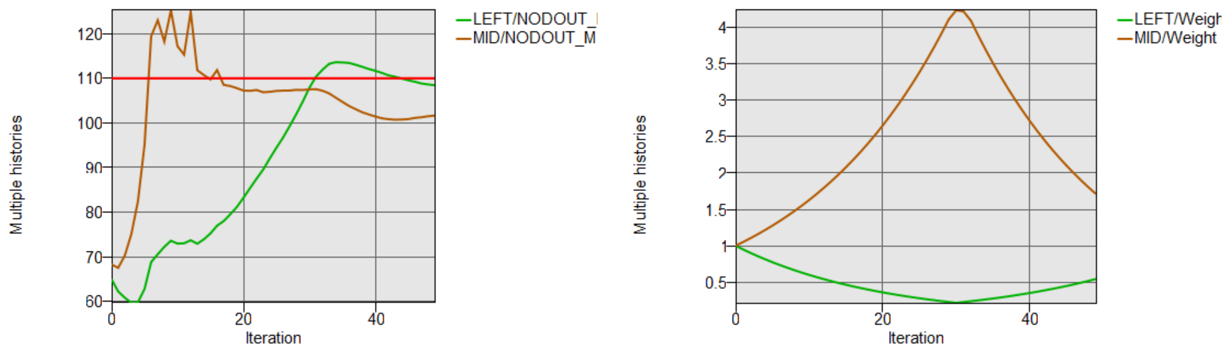

Figure 1-31: Constraint convergence history for multiple-load case example using dynamic weighting is shown on the left. Note the improvement with respect to not using dynamic weighting. The corresponding weight factors are shown on the right.

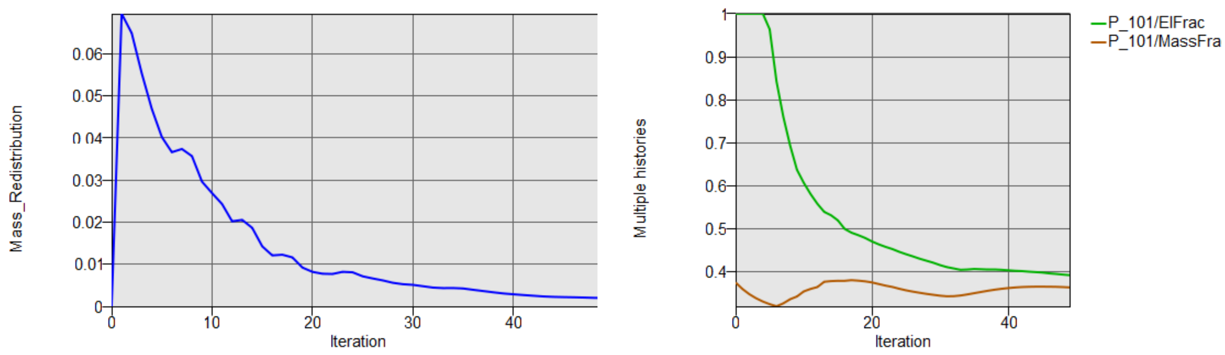

Figure 1-32: Various histories of the load case weight for multiple-load case example using dynamic weighting: mass redistribution, the fraction of elements kept, and the mass fraction.

The evolution of the topology under multiple loading conditions is shown in Figure 1-33. The final structure evolved in a tabular structure with the two cross-members as legs. The structure had more material in the center section due to the high importance assigned to the center weight. There were many cavities in the structure such that the final structure could be considered equivalent to a truss-like structure as one would expect.

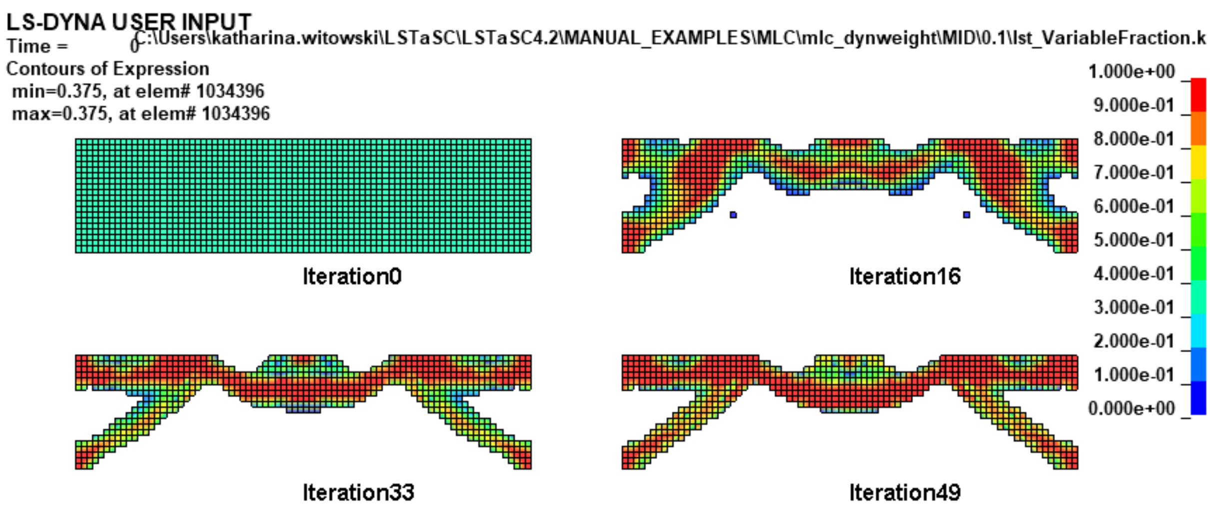

Figure 1-33: Evolution of the geometry for multiple-load case structure using dynamic scaling of the weights. The design is improved with respect to not using dynamic weighting by strengthening the portion of the structure carrying the center load.

1.5.4. Results using multi-point optimization

The optimization converged after 50 iterations, 3 simulations were performed per load case every other iteration. The results are as shown in Figure 1-34 to Figure 1-36.

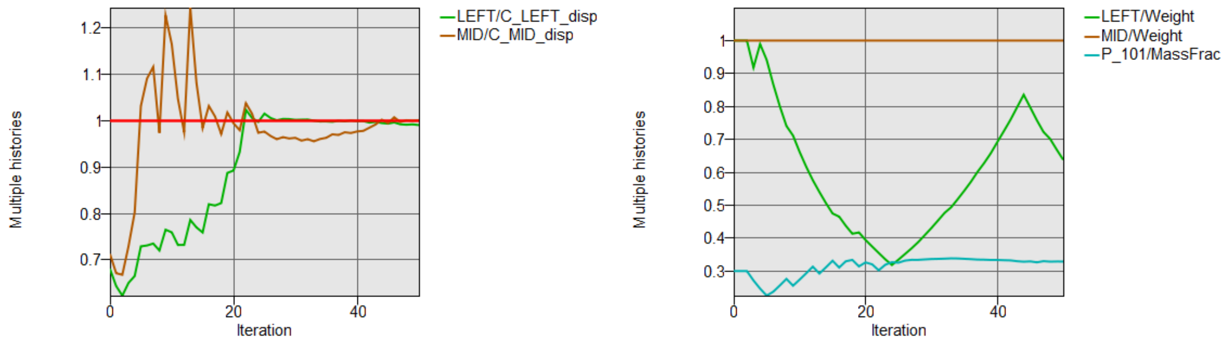

Figure 1-34: Constraint convergence history (left) and global variables (right) for constrained optimization with multiple load cases.

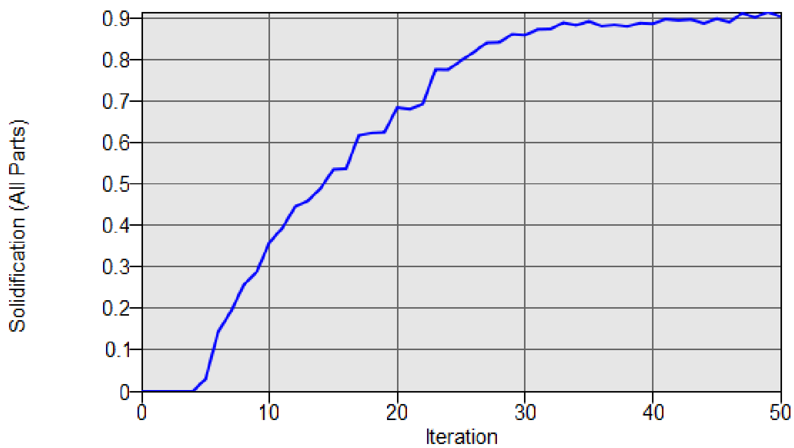

Figure 1-35: Solidification.

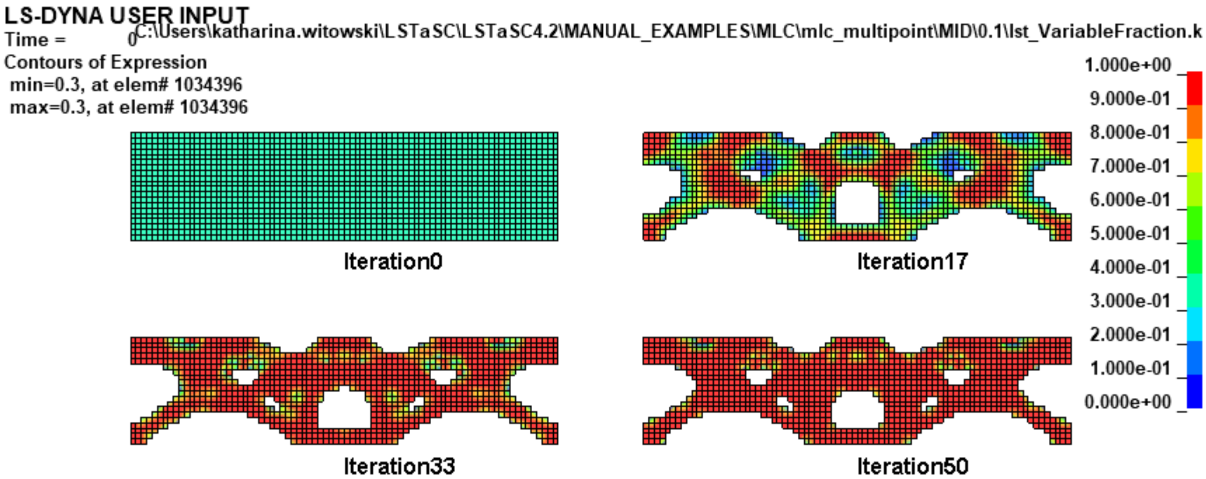

Figure 1-36: Evolution of the geometry for multiple-load case structure using multi-point method

1.6. Surface Design of a Beam

This example demonstrates:

- Free surface design for solids
- Extrusion and symmetry constraints for free surface design
- Smooth transition for free surface design

The related files are available in MANUAL/SURFACE/BEAM.

1.6.1. Problem Description

The geometry and loading conditions for the example are shown in Figure 1-37. The objective is to reduce stress concentrations using free surface design.

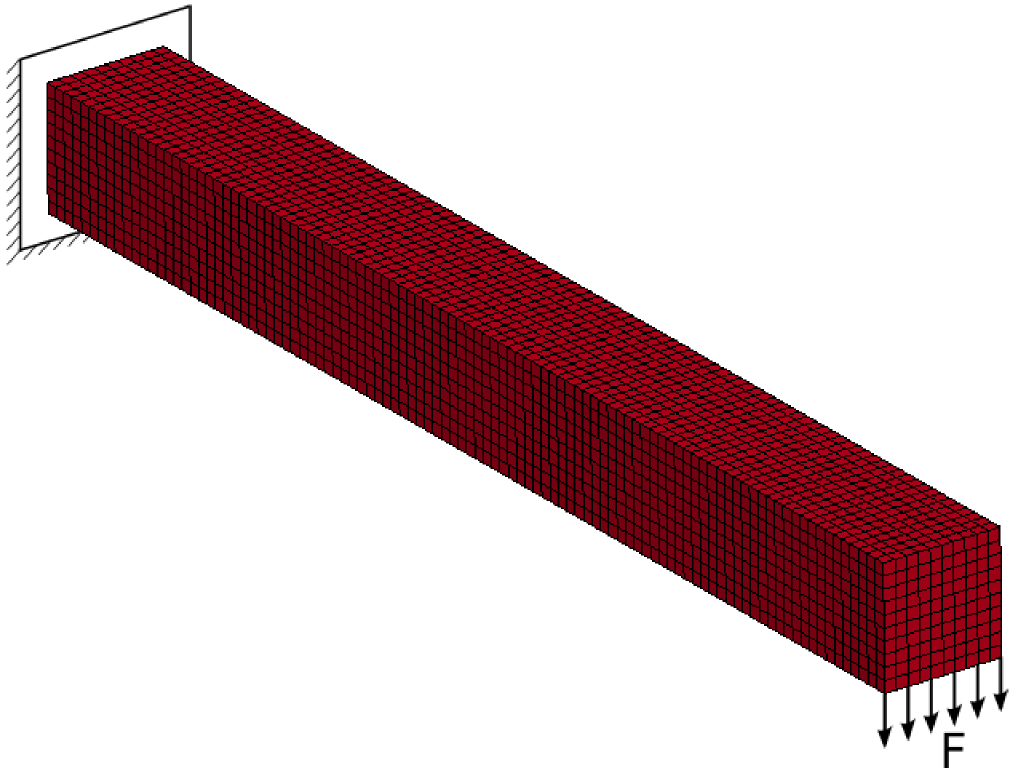

Figure 1-37: Beam model for free surface design

1.6.2. Problem Setup

To show various features of free surface design, four surfaces of the beam are optimized in the first example, in the second example, an extrusion and a symmetry constraint are defined, and in the third example, a smooth transition constraint is used.

The surface definition is displayed in Figure 1-38, Figure 1-39, and Figure 1-40, respectively. For the first two examples, the objective is to match the average stress, which is the default. The smooth transition example uses the minimize volume objective, which matches the maximal stress. Note that for the example with symmetry and extrusion constraints, the neighbor radius was increased to 0.5 to avoid a sharp structure.

The convergence tolerance for this example is a 50% smoothing of the stress, Figure 1-41.

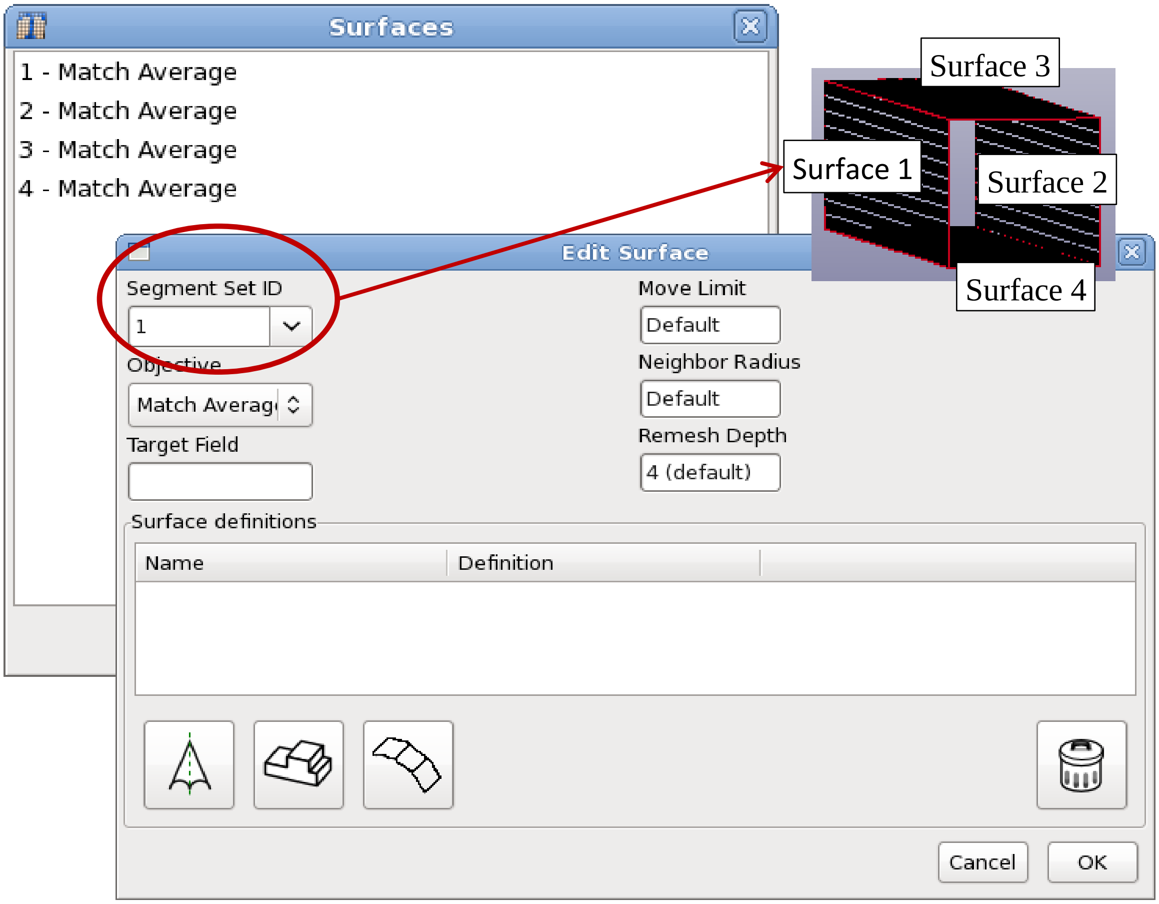

Figure 1-38: Definition of Surfaces; the objective is to match the average stress.

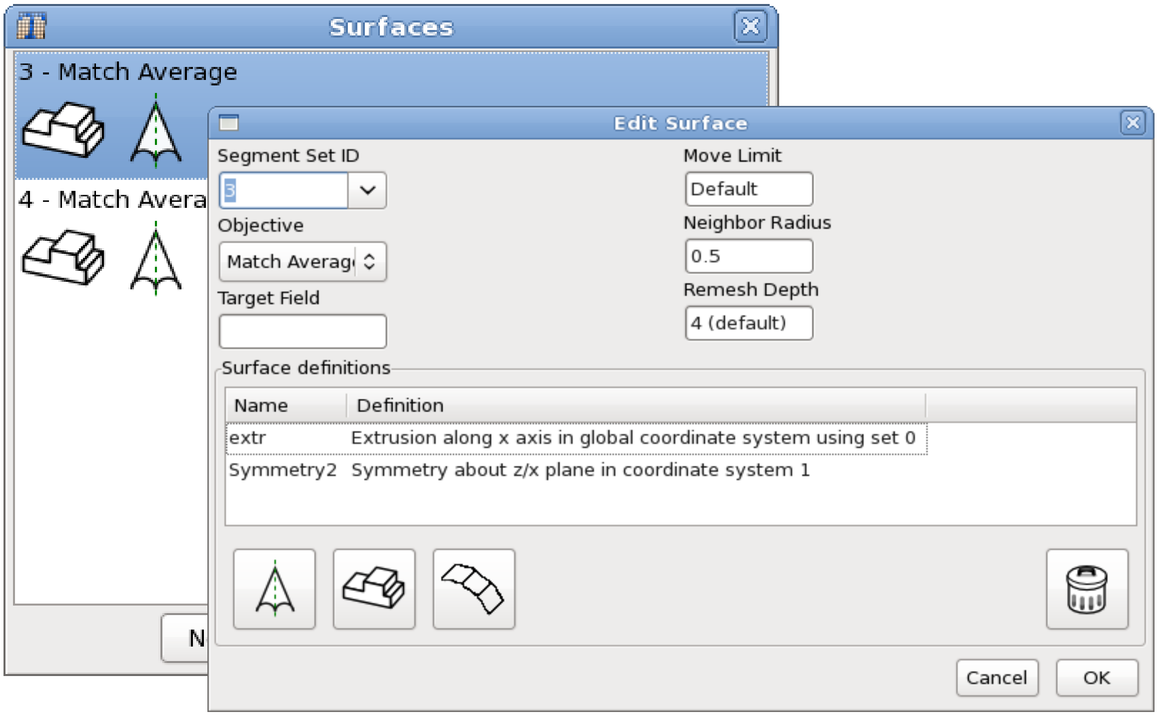

Figure 1-39: Definition of Surfaces with extrusion and symmetry constraint. To avoid a sharp geometry, the neighbor radius was increased to 0.5.

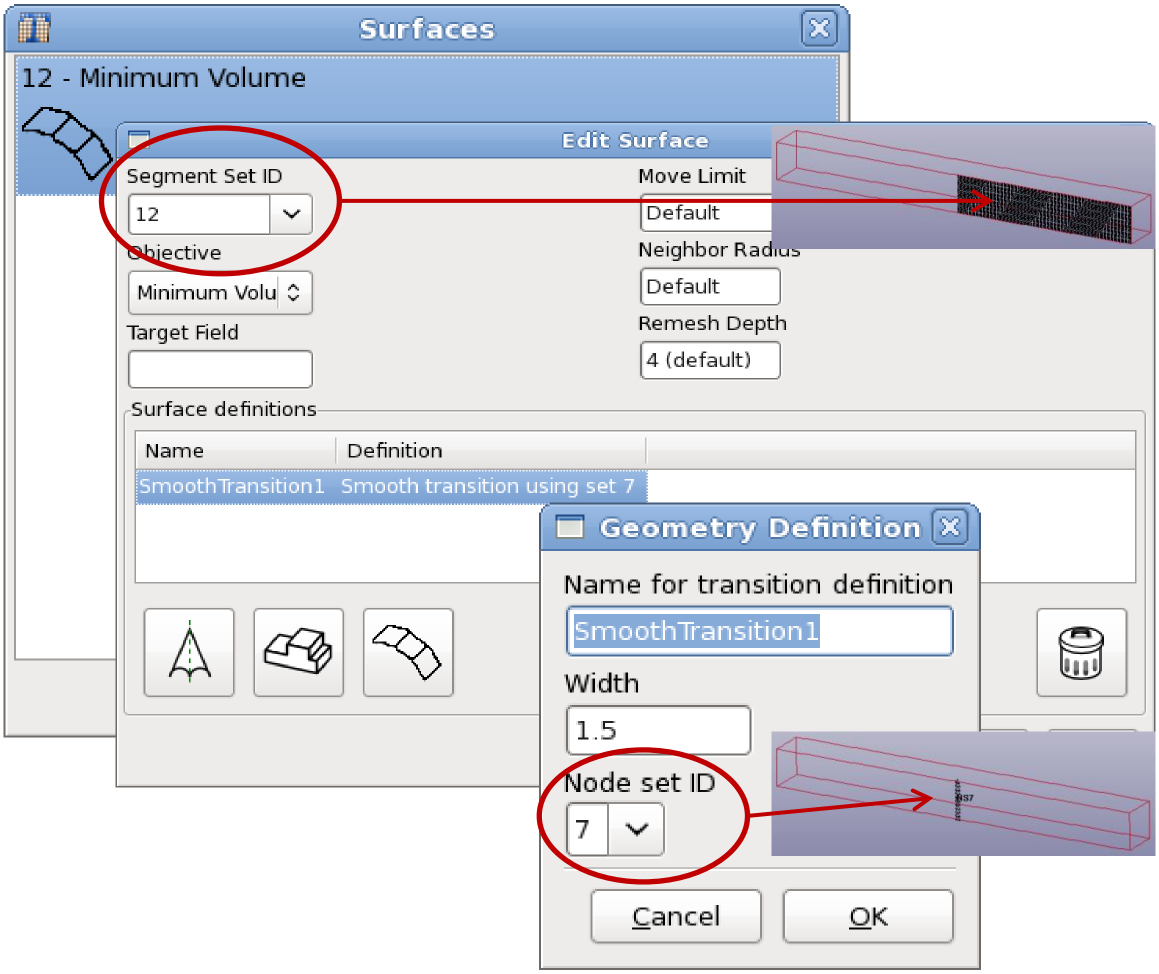

Figure 1-40: Surface with smooth transition definition. The objective is a minimum volume.

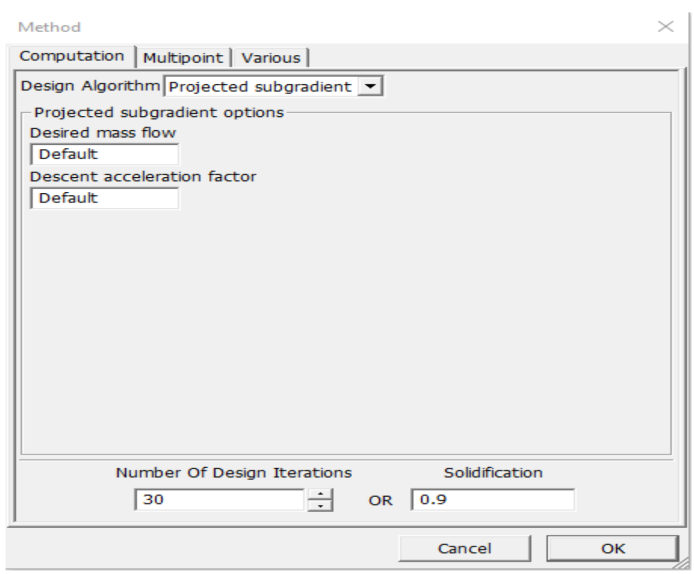

Figure 1-41: Termination criteria; the convergence tolerance is a 50% smoothing of the stress

1.6.3. Results with four surfaces

The project input data is saved to the file *all.lstasc* as provided in the examples distribution. All four sides of the beam were selected for shape design. The problem converged in 8 iterations. The initial and final design is displayed in Figure 1-42. Figure 1-43 shows the improvement of the stress smoothing.

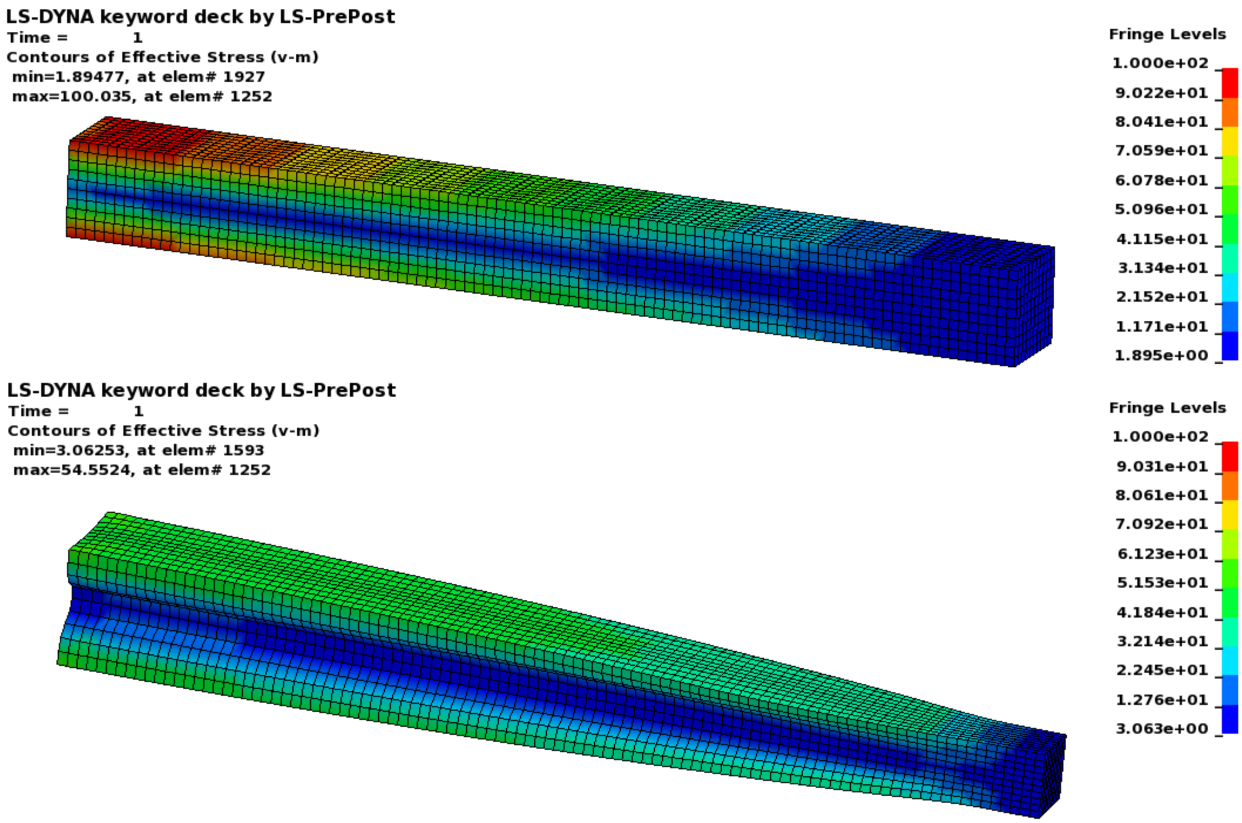

Figure 1-42: Initial and final design for four surfaces, Von Mises Stress fringed on the model

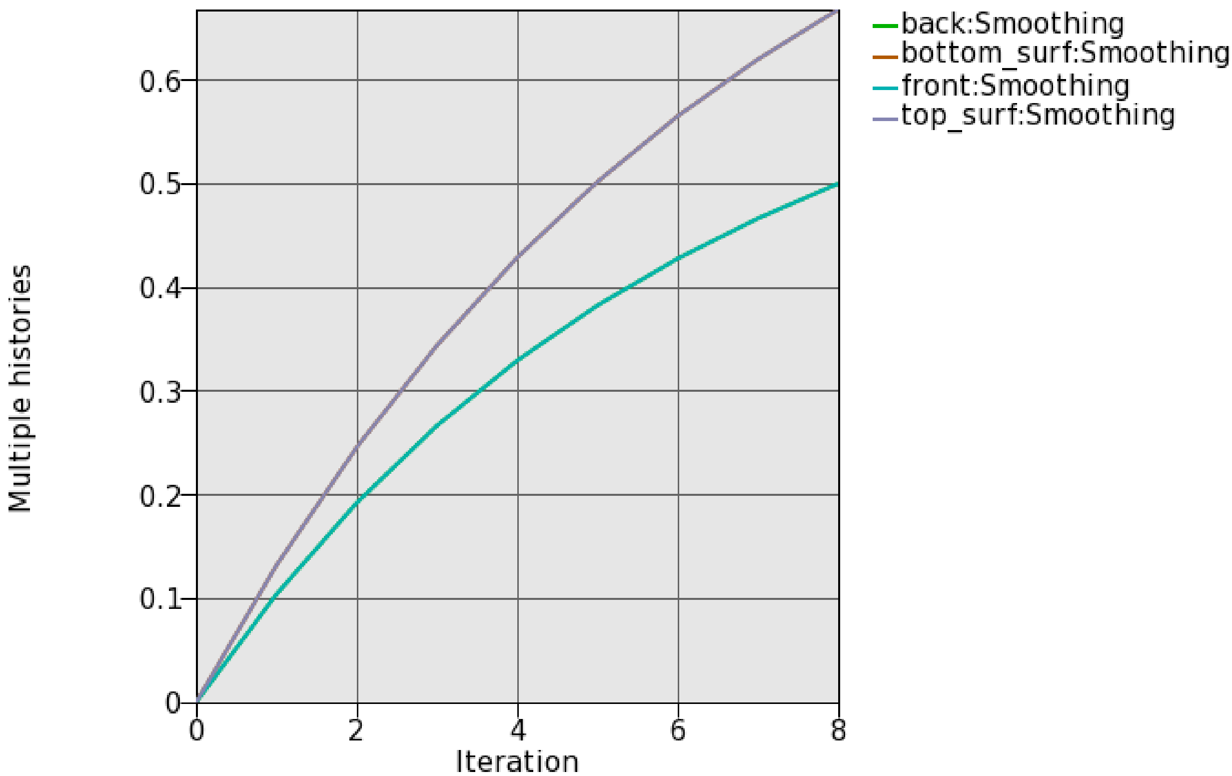

Figure 1-43: Convergence history; smoothing improvement of back/front and top/bottom

1.6.4. Results with extrusion and symmetry geometry definitions

The project input data is saved to the file *extr_symm.lstasc* as provided in the examples distribution. The front and back side of the beam were selected for shape design. The problem converged in 27 iterations. The initial and final design is shown in Figure 1-44. Note that for an extrusion such as this a complete smoothing of the stress is not possible, because the loading varies along the extrusion direction while the geometry does not. Figure 1-45 shows the improvement of the stress smoothing.

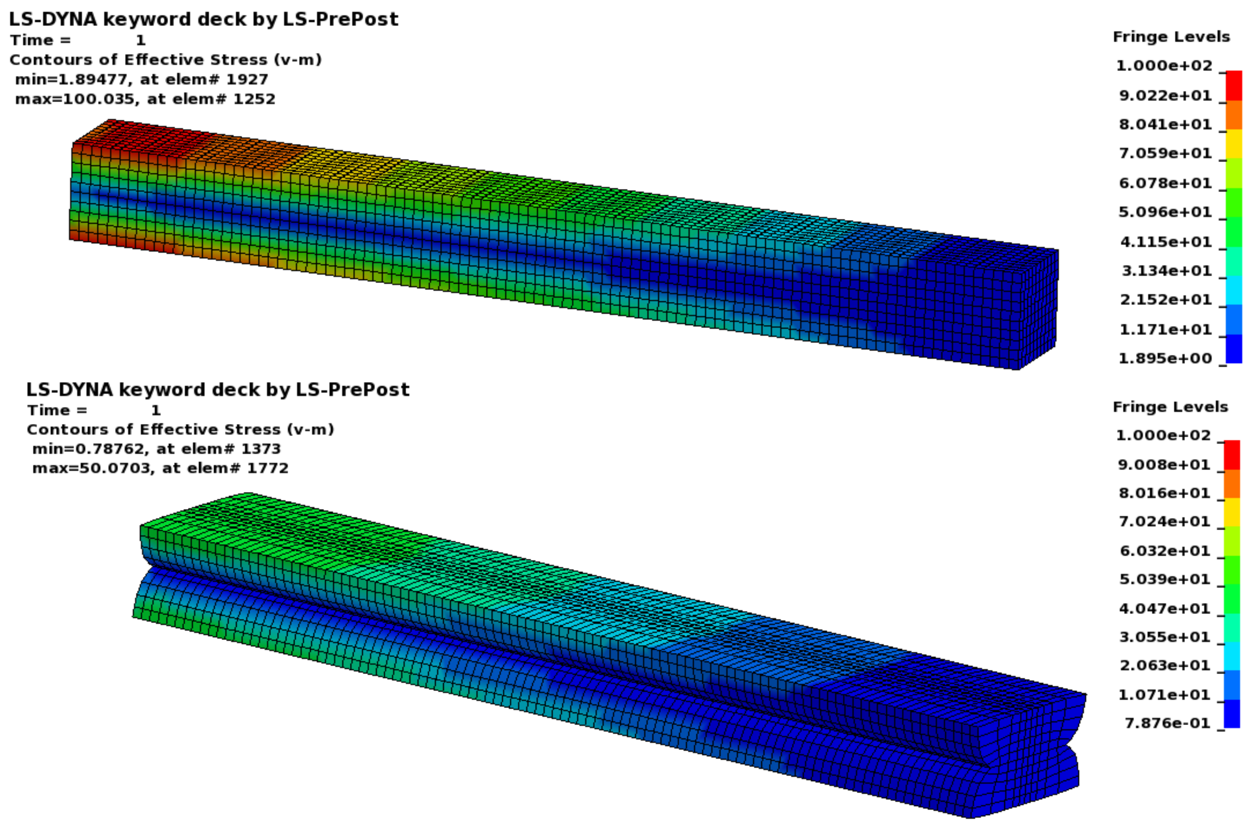

Figure 1-44: Initial and final design of beam with extrusion and symmetry geometry definitions with Von Mises stress fringed on model

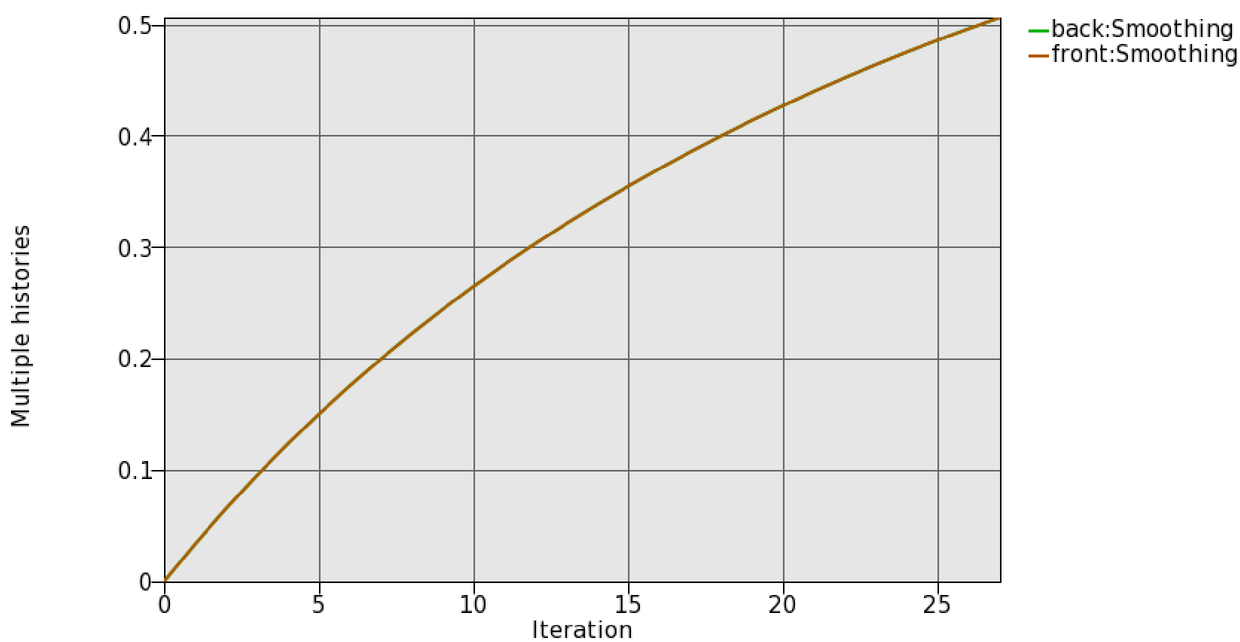

Figure 1-45: Convergence history of beam with extrusion and symmetry geometry definitions

1.6.5. *Results with smooth transition geometry definition*

The project input data is saved to the file *smooth_trans.lstasc* as provided in the examples distribution. The front half of the beam was selected for shape design. A node set was defined on the center edge and used to define the smooth transition, Figure 1-40. The objective was the minimum volume of the part. The initial and final design is as shown in Figure 1-46. The design without the smooth transition definition is shown in Figure 1-47 – the resulting poor mesh quality can be seen.

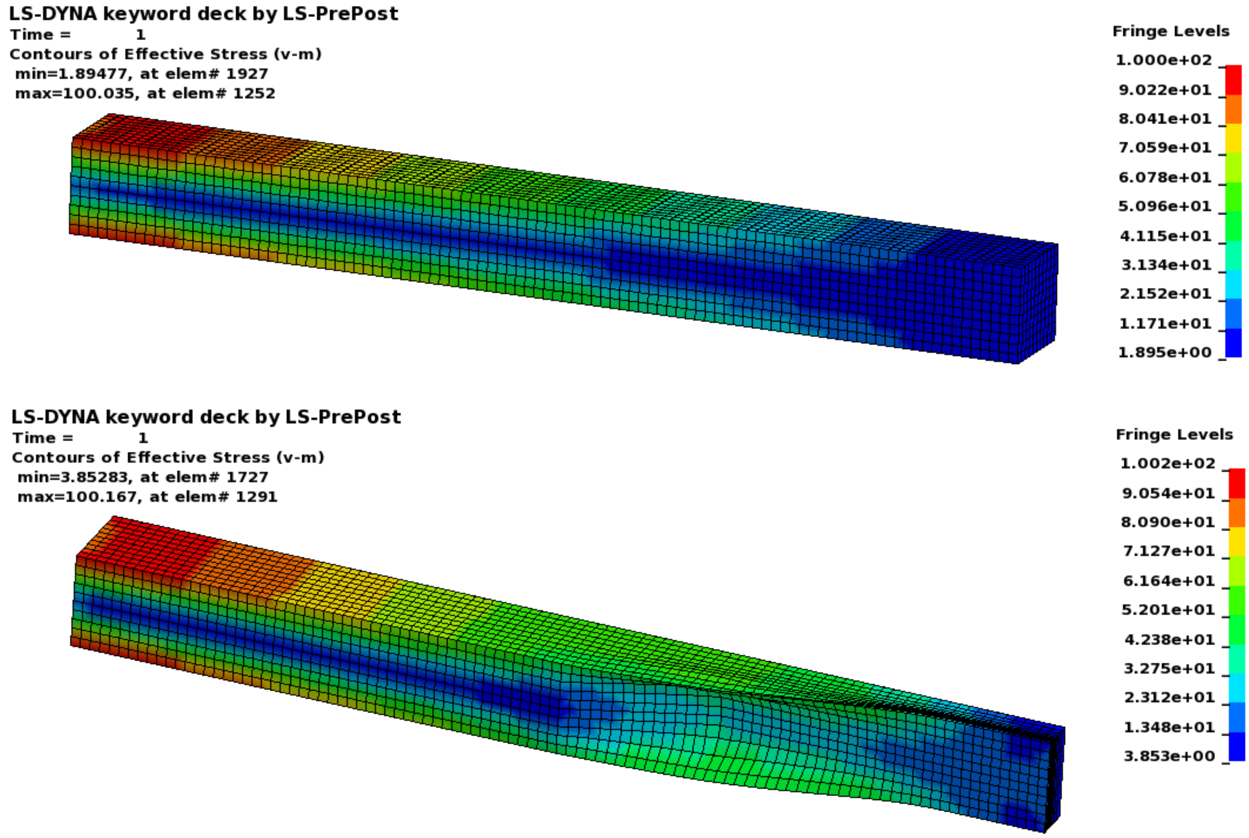

Figure 1-46: Initial and final design of beam with smooth transition geometry definition

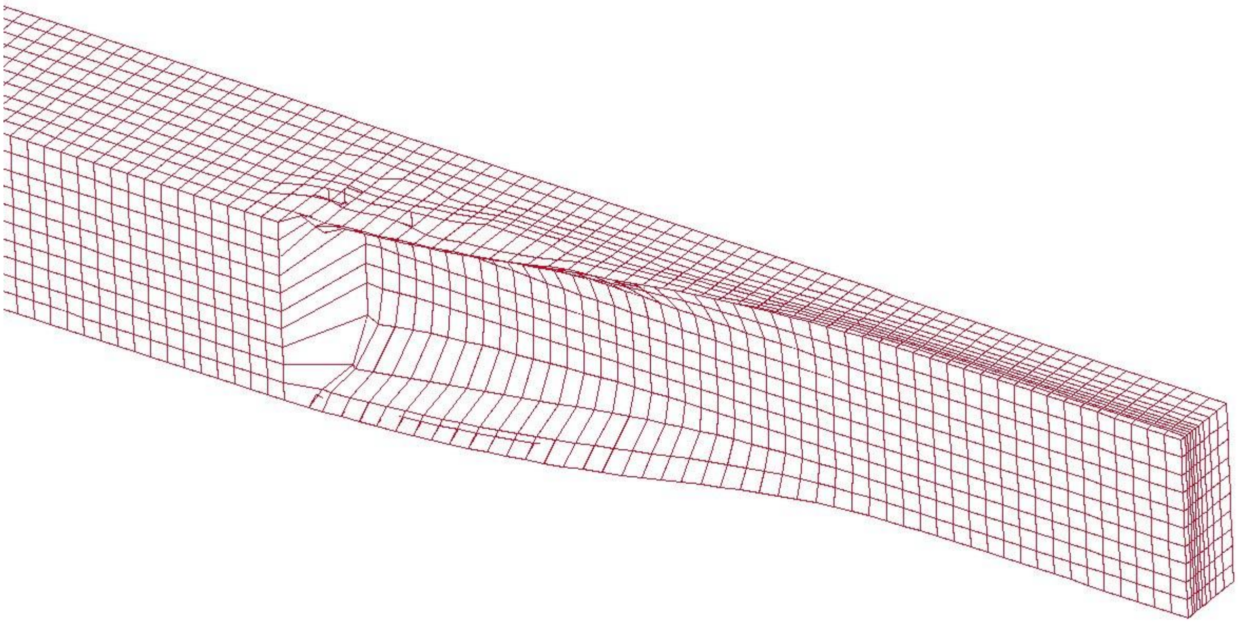

Figure 1-47: Design of beam without smooth transition geometry definition

1.7. Fundamental frequency and multidisciplinary problems

This example demonstrates

- topology optimization of fundamental frequency and multi-disciplinary optimization (MDO) problems using the Projected Subgradient Decent method,
- topology optimization for a single loading case of the NVH design, and
- topology optimization for MDO with combined statics and NVH design, and
- topology optimization for MDO with multiple constraints.

The related files are available in MANUAL/EIGEN_MDO.

1.7.1. Problem Description

The geometry is a beam with dimensions of 8 mm × 1 mm × 0.5 mm, as shown in Figure 1-48. A load of 10 units is applied at the center of the beam. The meshed geometry and boundary condition in x-y plane are shown in Figure 1-49. The design part was meshed with (0.03125 mm)^2 × 0.5 mm elements.

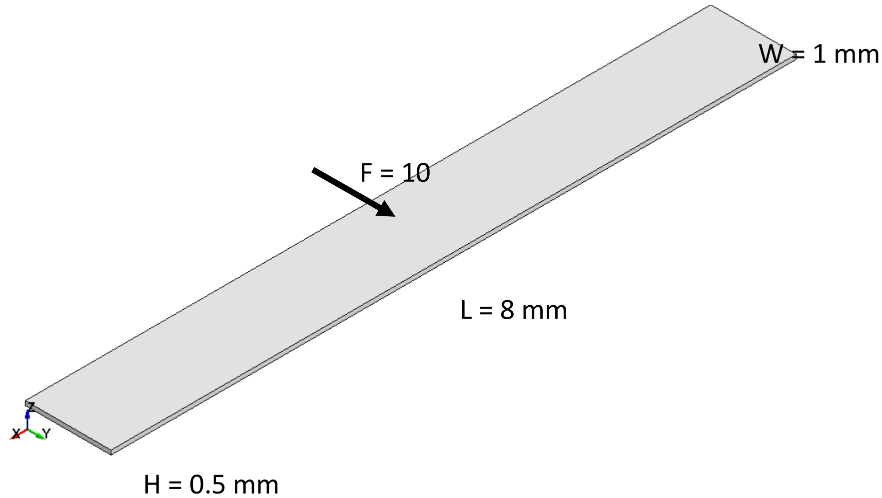

Figure 1-48: The geometry and boundary condition of the MDO example.

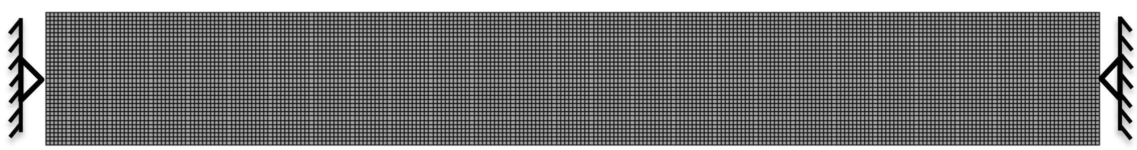

Figure 1-49: Geometry and boundary condition of the MDO example.

1.7.2. Problem Setup

As provided in the examples distribution directory MDO, the definition of meshing the geometry is saved to the file *mesh.k*, and it is read by the statics and NVH load cases. The linear statics load case is defined in the file *load.k*, and the NVH load case is defined in the file *freq_bc1.k*.

NVH design: The input data for topology optimization of the beam structure under a single loading case of the NVH design is saved to the file *freq.lstasc* as provided in the examples distribution. The project is to seek for the best design of the beam structure with the maximum first eigenfrequency. The definition of Case "*Frequency"* is displayed in Figure 1-50. Selection of different boundary conditions can be done by browsing the "*Input file name*" and choosing the keyword file of the boundary condition of interest. The definition of the design part is displayed in Figure 1-51. The desired mass fraction for this example was 0.5. In the *Method* dialog *Computation* tab, a maximum of 100 iterations or a Solidification value of 0.9 were allowed, as shown in Figure 1-52. In *Various* tab, four schemes can be used to deal with the *Unconnected regions*, including "*Ignore*", "*Warn*", "*Delete*", and "*Delete small*". In this example, the scheme of "*Delete small*" is selected. In the tag of *Solid/Void strategy* that includes "*True mechanics*", "*SIMP*", and "*Gradual SIMP*", "*SIMP*" approach is selected for the MDO design. Parameter for "*SecondFreqGap*" is set as "-0.15", meaning that a constraint of 15% distance is applied on the gap between the first and second frequencies.

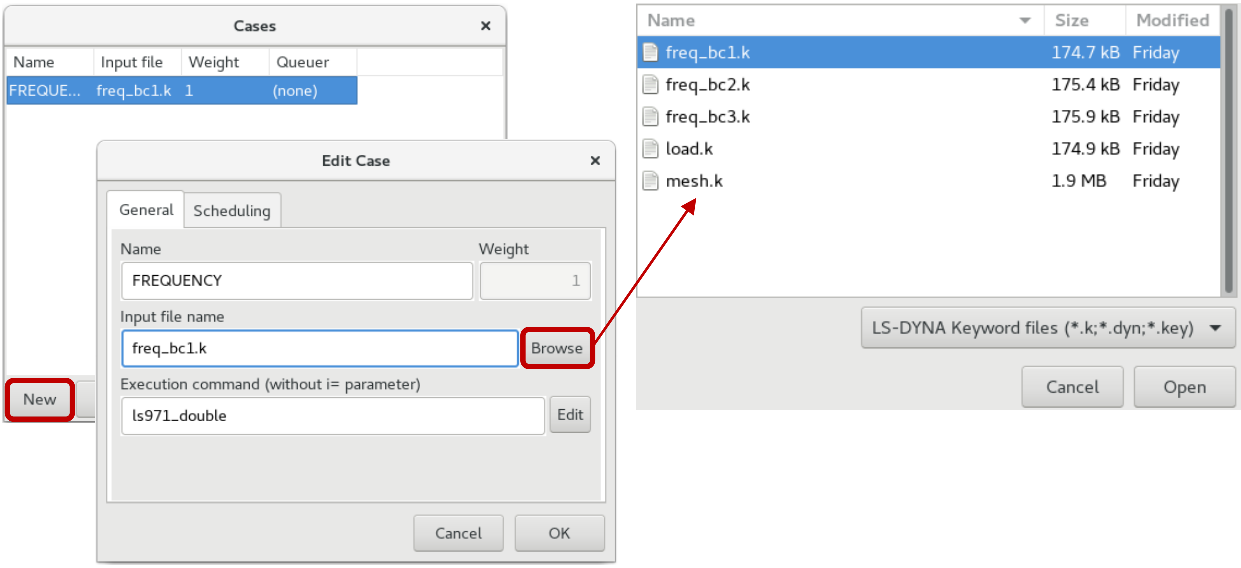

Figure 1-50: Definition of NVH design with boundary condition of interest.

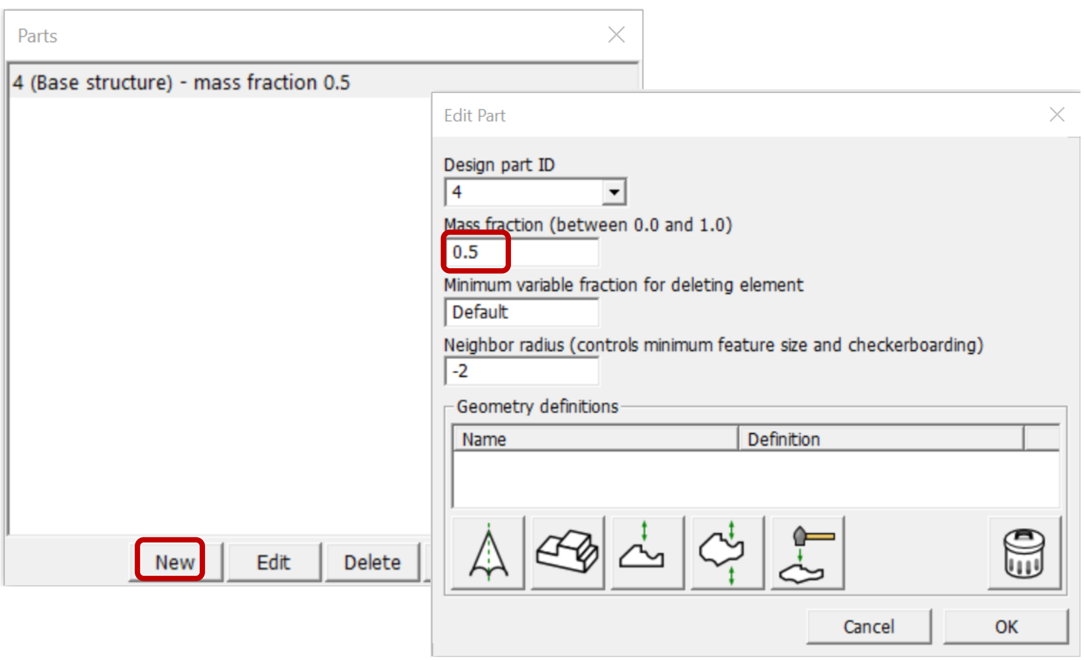

Figure 1-51: Design part definition of NVH design with desired mass fraction 0.5.

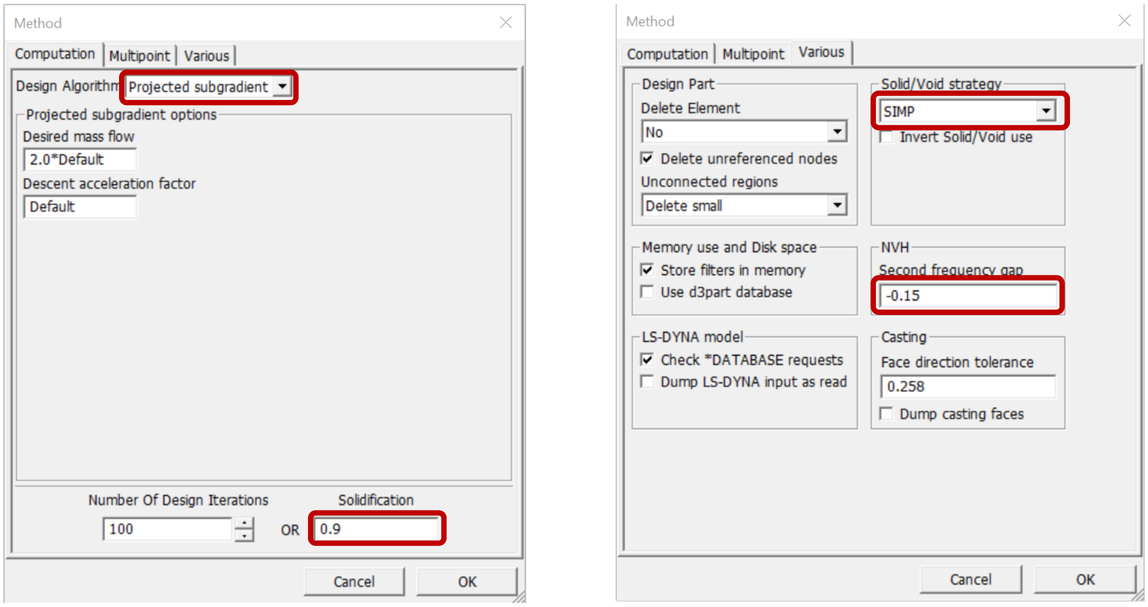

Figure 1-52: Setting of termination criteria and solid/void strategy for NVH design.

MDO with combined statics and NVH load cases: The input data for topology optimization of the beam structure under multiple loading cases of combined statics and NVH design is saved to the file *mdo.lstasc*. The project is to seek for the best design of the beam structure, which has the maximum first eigenfrequency in the NVH design and is the stiffest structure in a statics load. The definition of multiple load cases, Case "FREQUENCY" and Case "LOAD", is displayed in Figure 1-53. Constant weights for each load case are defined in the Cases definition as well. Similar to the single load case of NVH design, different boundary conditions can be selected for the design. The definition of the design part and setting for Method dialog are similar to the settings in the previous problem.

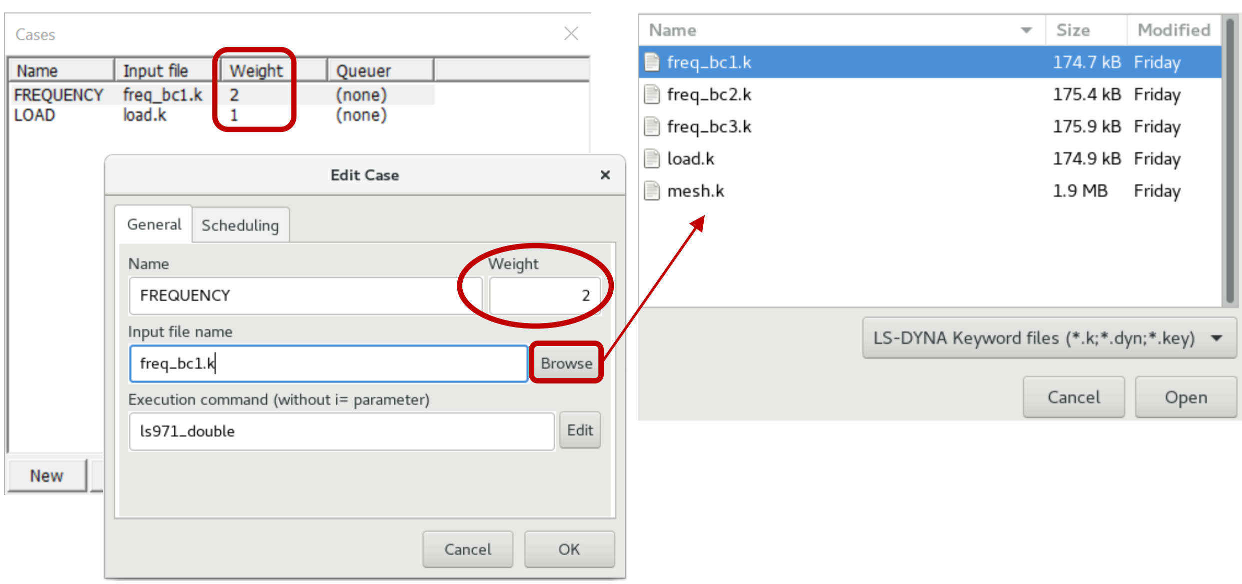

Figure 1-53: Definition of multiple load cases with constant weights and boundary condition.

MDO with multiple constraints: The input data for topology optimization of the beam structure for mass minimization with two frequency and a displacement constraints is saved to the file *mdo_con.lstasc*. The constraints are applied on the frequency of the 2nd and 3rd eigenmodes of the baseline design. The definition of objective and constraint is set up as shown in Figure 1-54. Since the 2nd and 3rd eigenmodes are the mode of interest in the design, the "Mode Tracking" is set as "On" to track the target modes. The setting for Method dialog is shown in Figure 1-55, where the constraints are normalized because of large difference between constraint bounds, and constraint DSA is computed every two iterations since the third iteration by using the central difference scheme. The definition of the design part is similar to the settings in the previous problem.

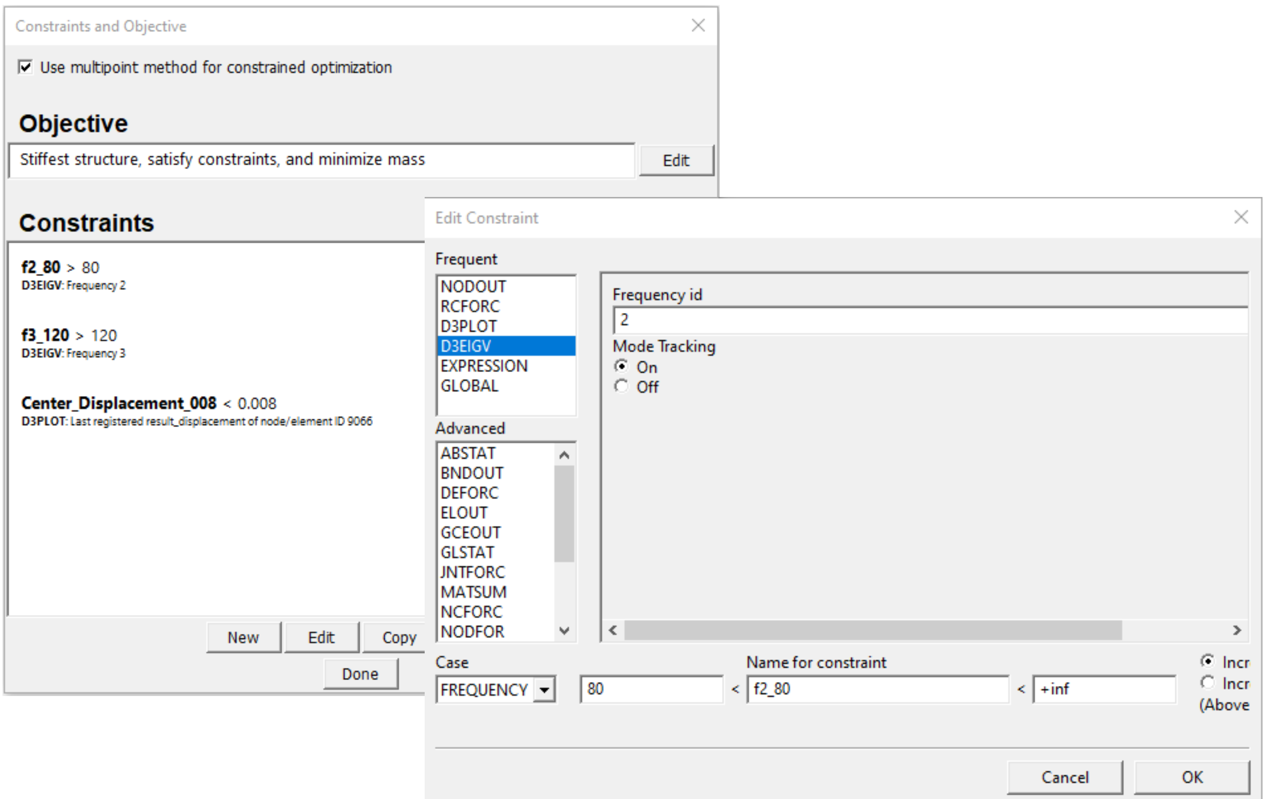

Figure 1-54: Optimization problem definition for MDO with multiple constraints.

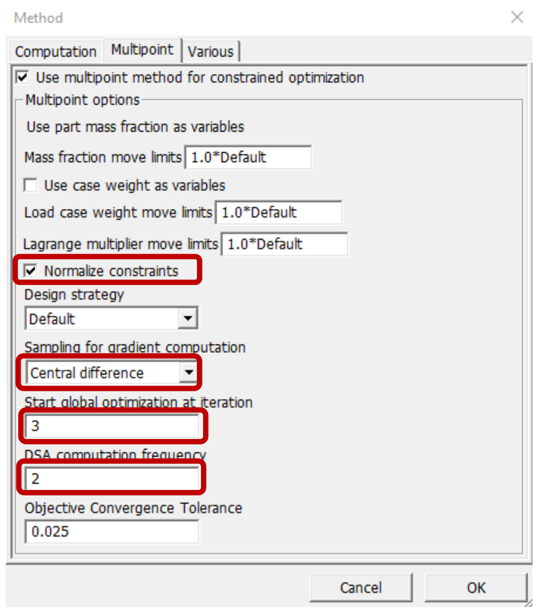

Figure 1-55: Setting of Method dialog for MDO with multiple constraints.

1.7.3. Results with a single load case of NVH design

The optimization converged after 48 iterations. The convergence history for the example with a single NVH design is shown in Figure 1-56. The base and second eigenfrequencies of the final optimized structure are, respectively, 26.15 Hz and 35.90 Hz. The evolution of the topology of the beam for a single NVH design is shown in Figure 1-57. The final structure had many cavities in Figure 1-58.

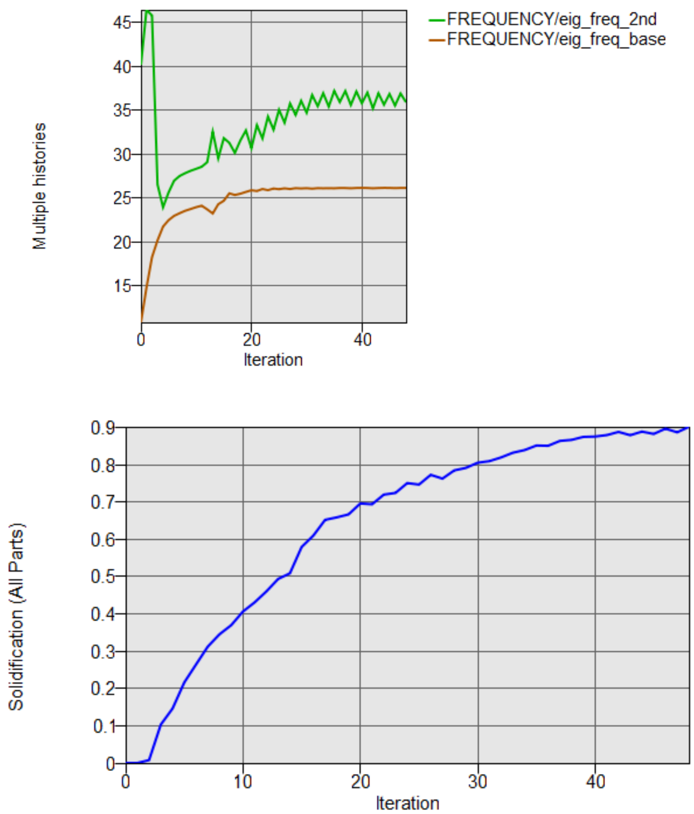

Figure 1-56: Convergence history for the example with NVH design, the first two eigenfrequencies (upper) and Solidification (bottom).

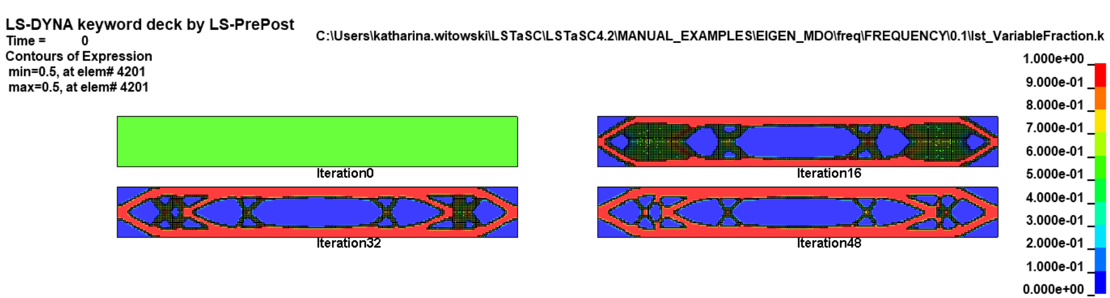

Figure 1-57: Evolution of the geometry for NVH design.

Figure 1-58: Final geometry for NVH design: iso-surface with iso-level 0.3.

1.7.4. Results of MDO with combined statics and NVH load cases

The optimization converges after 32 iterations. The results of the beam with combined statics and NVH load cases are as shown in Figure 1-59 to Figure 1-60. The base and second eigenfrequencies of the final optimized structure are, respectively, 25.86 Hz and 39.59 Hz. The displacement at the loading point on the optimized structure is approximately 0.00961m. History of design contributions history of two load cases and Solidification are shown in Figure 1-61. The evolution of the topology of the beam with combined statics and NVH load cases is shown in Figure 1-62. The final structure in Figure 1-63 had many cavities.

The contributing case of two load cases on the beam structure is plotted in Figure 1-64. Note that the material contributing to different load cases is shown with binary numbers in the color bar. For example, a value of 1 (0001 in binary) means that material is used by load case 1, and a value of 2 (0010 in binary) means that material is used by load case 2, and a value of 3 (0011 in binary) means that it is used by both load cases. Specifically, in this example, the parts in green color indicate active parts in the first load case "FREQUENCY", the NVH load case. The parts in yellow color indicate active parts in the second load case "LOAD", the linear statics load case. The parts in red color indicate active parts in both load cases.

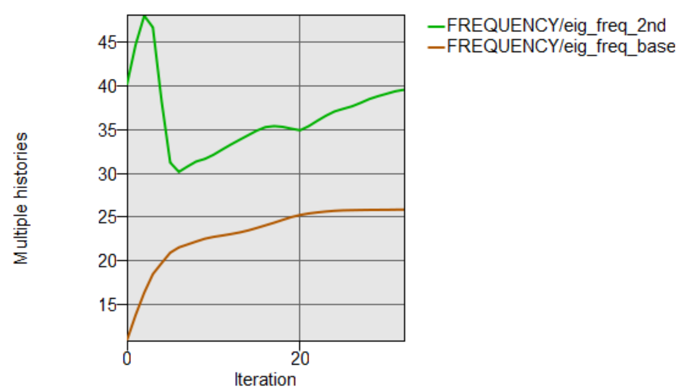

Figure 1-59: First two eigenfrequencies convergence history for MDO.

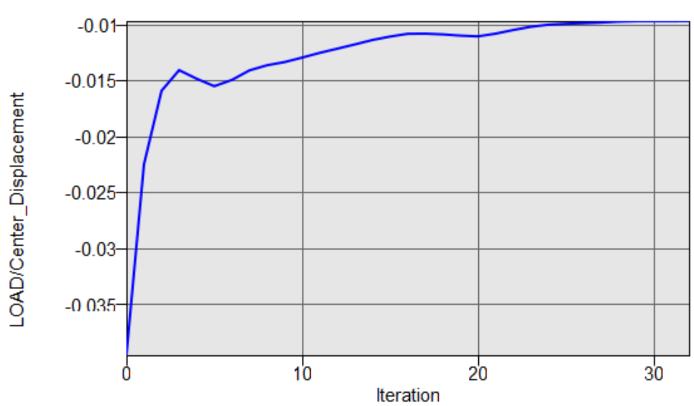

Figure 1-60: displacement at the loading point for MDO.

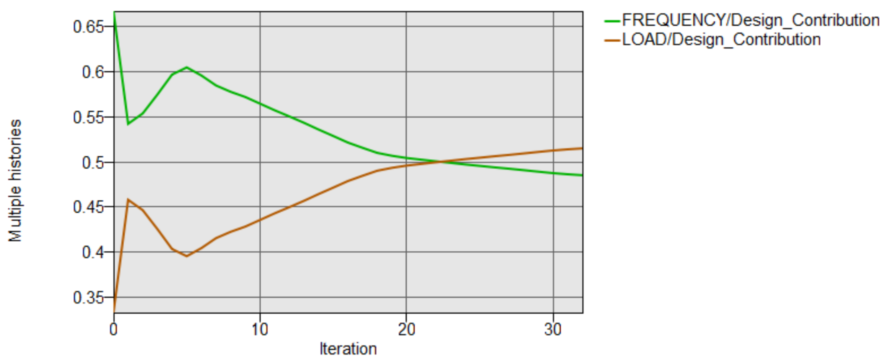

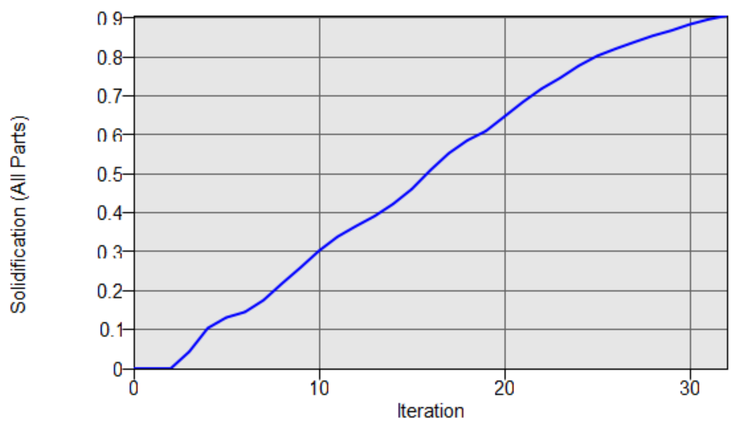

Figure 1-61: History of design contributions history of two load cases (upper) and Solidification (bottom) for MDO.

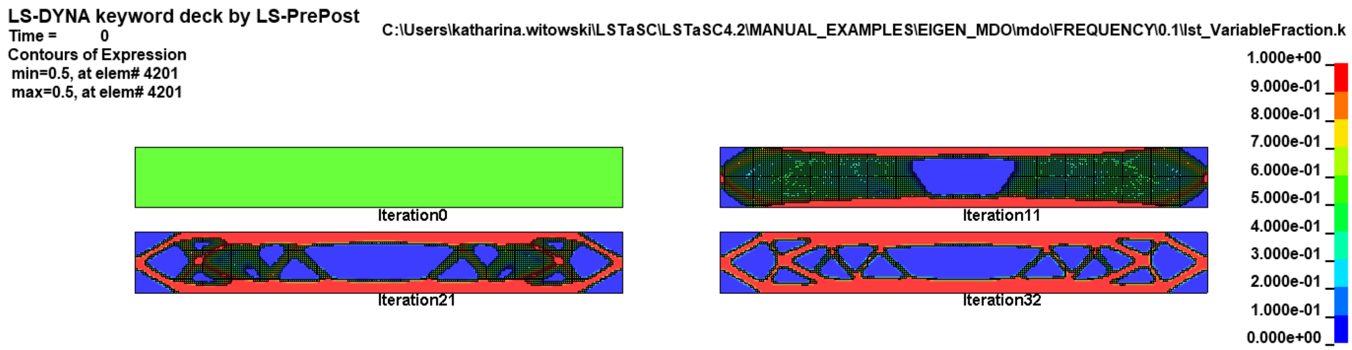

Figure 1-62: Evolution of the geometry for MDO.

Figure 1-63: Final beam structure for MDO: iso-surface with iso-level 0.3.

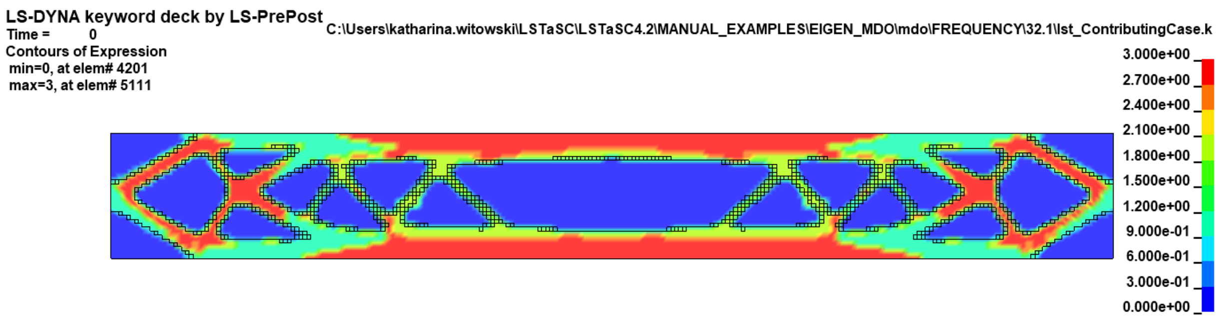

Figure 1-64: Contributing case for MDO.

1.7.5. Results of MDO with multiple constraints

The optimization converges after 39 iterations. The results of optimization histories of fundamental eigenfrequency and constrained frequencies, as well as the mode tracking history of the target eigenmodes, are as shown in Figure 1-65. The base and second eigenfrequencies of the final optimized structure are, respectively, 24.41 Hz and 79.94 Hz. The frequency constraints on the 2nd and 3rd eigenmodes of the based structure are satisfied in the optimization process. The histories of structural mass (objective) and displacement constraint are shown in Figure 1-66.

History of Solidification is shown in Figure 1-67, and history of the contributing case of two load cases is plotted in Figure 1-68. The evolution of the topology of the beam with a frequency constraint on a target eigenmode is shown in Figure 1-69. The final structure is shown in Figure 1-70.

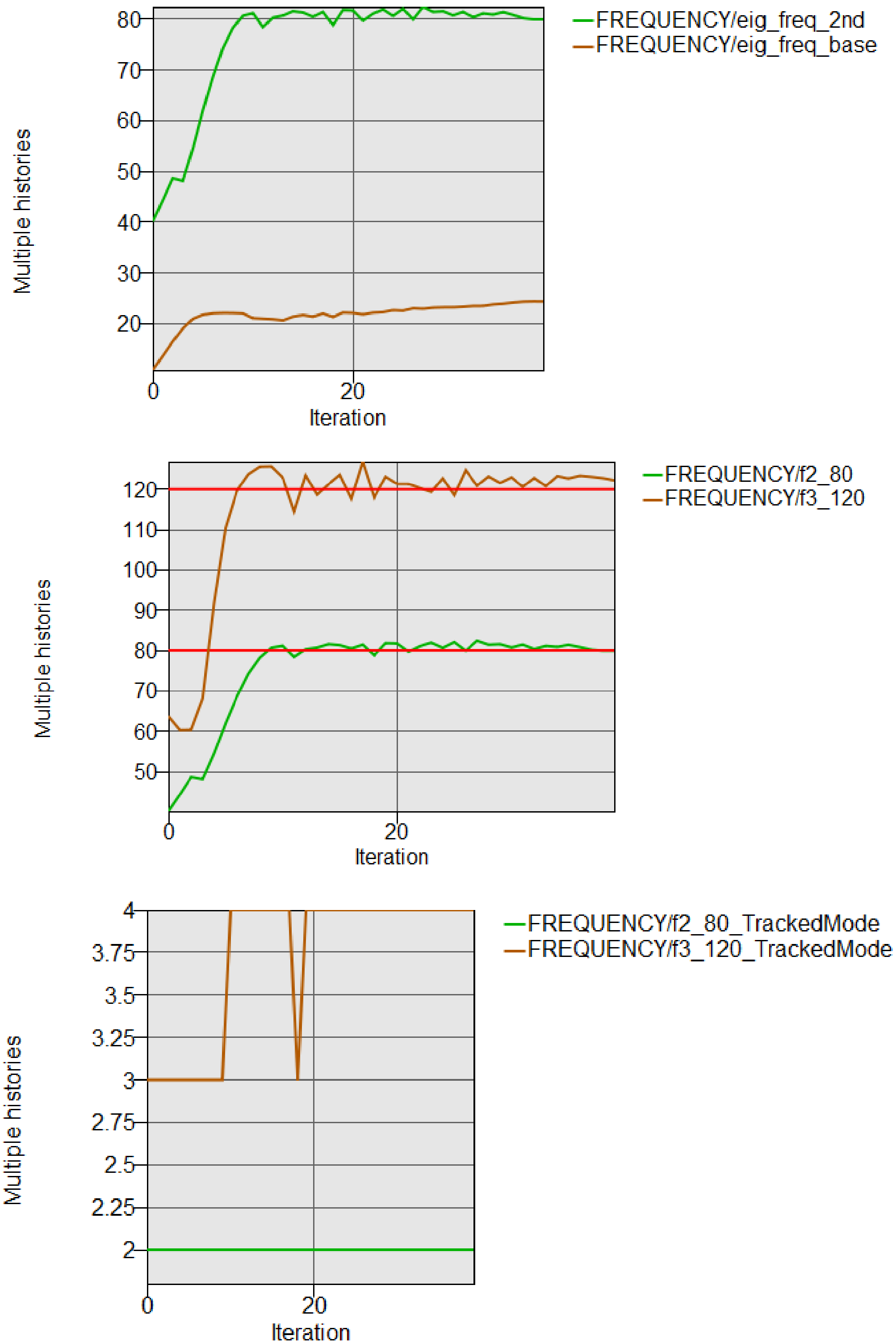

Figure 1-65: First two eigenfrequencies convergence history (upper), frequency constraints (middle), and mode tracking history of target eigenmodes (bottom).

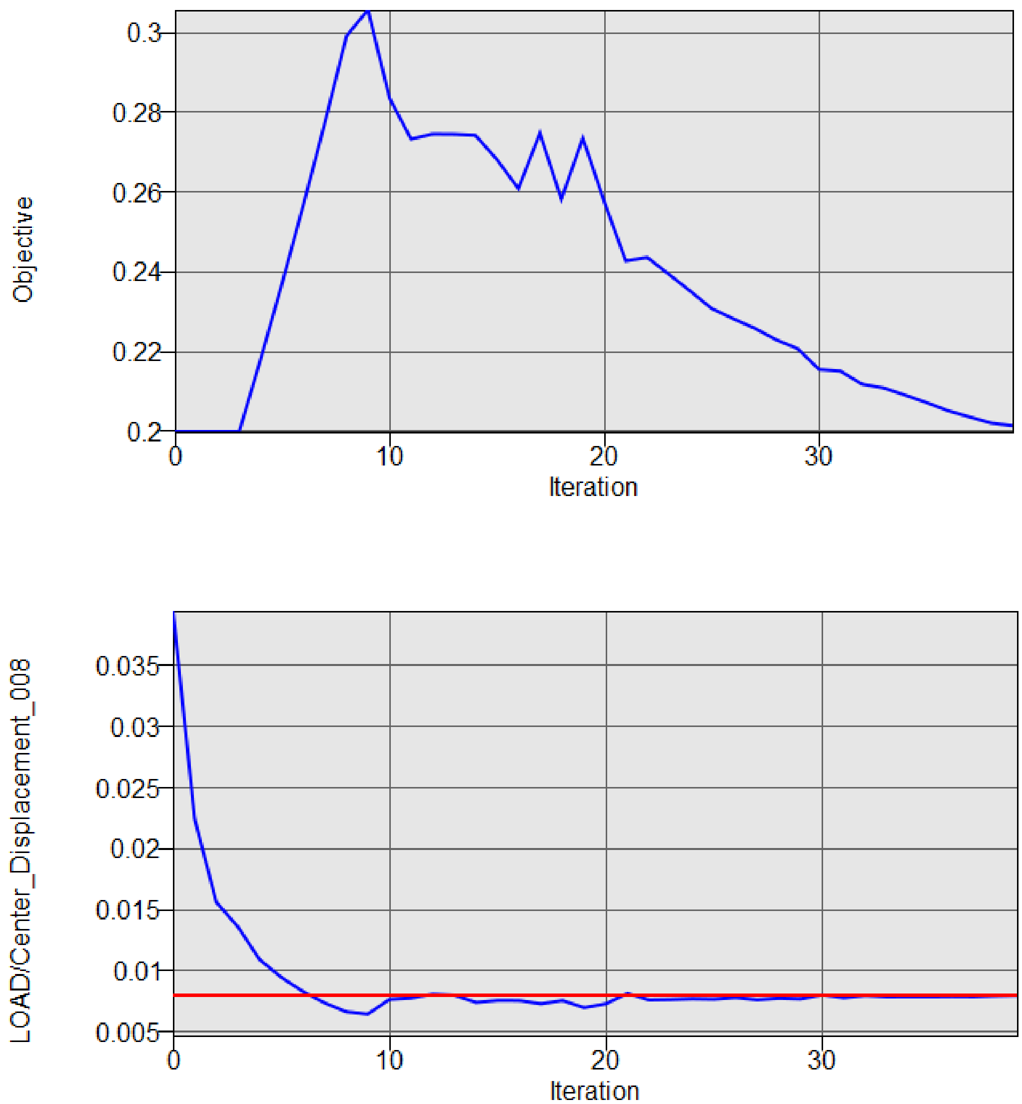

Figure 1-66: Histories of structural mass (upper) and the displacement constraint (bottom).

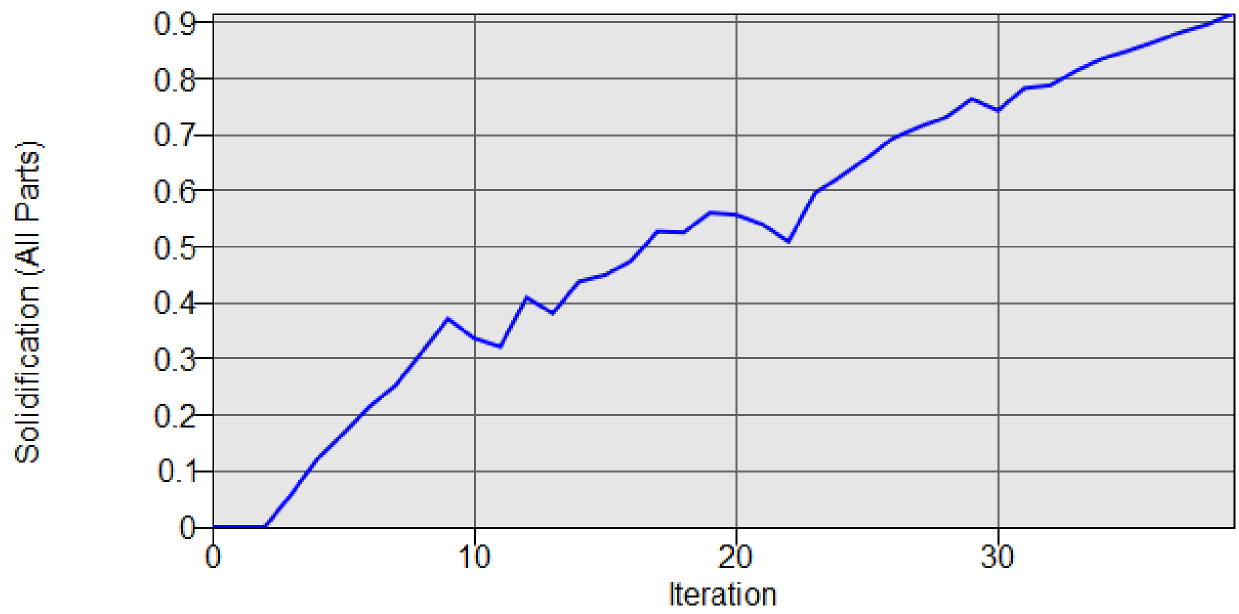

Figure 1-67: History of Solidification.

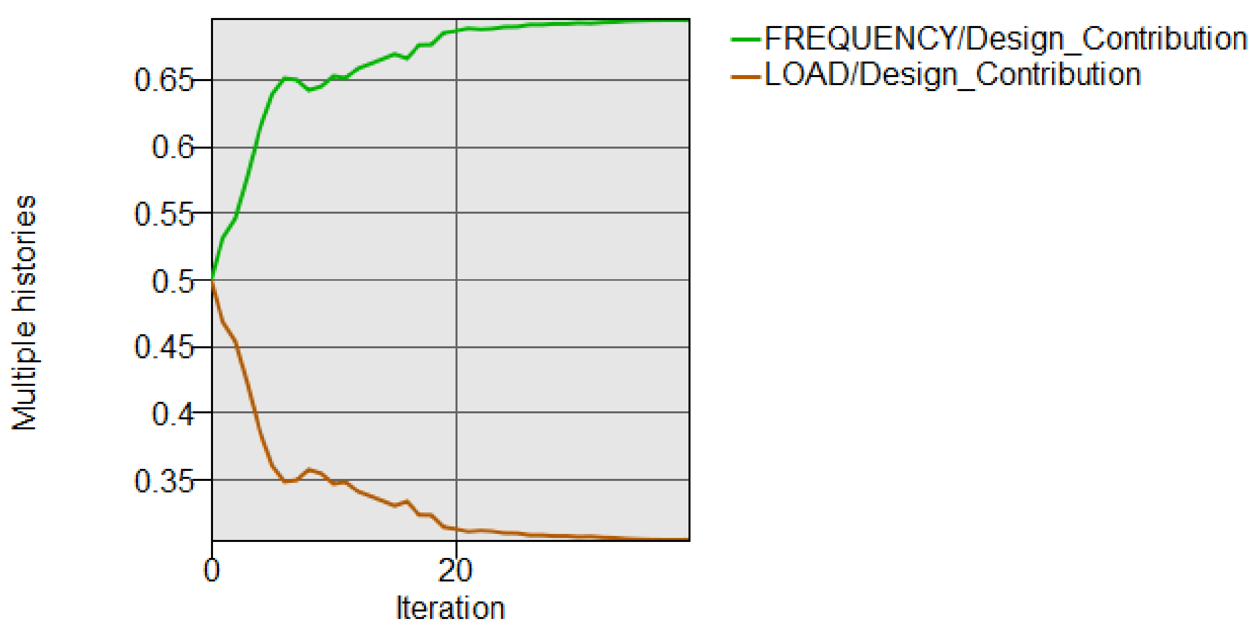

Figure 1-68: History of Contributing Cases.

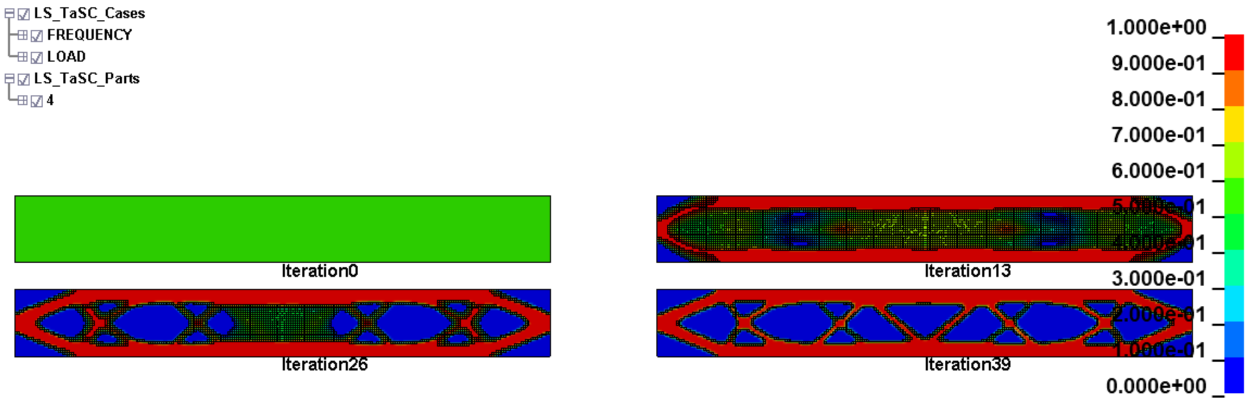

Figure 1-69: Evolution of the geometry for MDO with multiple constraints.

Figure 1-70: Final beam structure for MDO with multiple constraints: iso-surface with iso-level 0.3.